

Identification of specific sources of airborne particles emitted from within a complex industrial (steelworks) site

Beddows, David; Harrison, Roy

DOI:

[10.1016/j.atmosenv.2018.03.055](https://doi.org/10.1016/j.atmosenv.2018.03.055)

License:

Creative Commons: Attribution-NonCommercial-NoDerivs (CC BY-NC-ND)

Document Version

Peer reviewed version

Citation for published version (Harvard):

Beddows, D & Harrison, R 2018, 'Identification of specific sources of airborne particles emitted from within a complex industrial (steelworks) site', *Atmospheric Environment*, vol. 183, pp. 122-134.
<https://doi.org/10.1016/j.atmosenv.2018.03.055>

[Link to publication on Research at Birmingham portal](#)

Publisher Rights Statement:

Checked for eligibility: 13/04/2018

<https://www.sciencedirect.com/science/article/pii/S1352231018302176>

<https://doi.org/10.1016/j.atmosenv.2018.03.055>

General rights

Unless a licence is specified above, all rights (including copyright and moral rights) in this document are retained by the authors and/or the copyright holders. The express permission of the copyright holder must be obtained for any use of this material other than for purposes permitted by law.

- Users may freely distribute the URL that is used to identify this publication.
- Users may download and/or print one copy of the publication from the University of Birmingham research portal for the purpose of private study or non-commercial research.
- User may use extracts from the document in line with the concept of 'fair dealing' under the Copyright, Designs and Patents Act 1988 (?)
- Users may not further distribute the material nor use it for the purposes of commercial gain.

Where a licence is displayed above, please note the terms and conditions of the licence govern your use of this document.

When citing, please reference the published version.

Take down policy

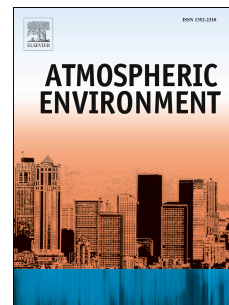
While the University of Birmingham exercises care and attention in making items available there are rare occasions when an item has been uploaded in error or has been deemed to be commercially or otherwise sensitive.

If you believe that this is the case for this document, please contact UBIRA@lists.bham.ac.uk providing details and we will remove access to the work immediately and investigate.

Accepted Manuscript

Identification of specific sources of airborne particles emitted from within a complex industrial (steelworks) site

D.C.S. Beddows, Roy M. Harrison



PII: S1352-2310(18)30217-6

DOI: [10.1016/j.atmosenv.2018.03.055](https://doi.org/10.1016/j.atmosenv.2018.03.055)

Reference: AEA 15925

To appear in: *Atmospheric Environment*

Received Date: 31 August 2017

Revised Date: 9 March 2018

Accepted Date: 27 March 2018

Please cite this article as: Beddows, D.C.S., Harrison, R.M., Identification of specific sources of airborne particles emitted from within a complex industrial (steelworks) site, *Atmospheric Environment* (2018), doi: 10.1016/j.atmosenv.2018.03.055.

This is a PDF file of an unedited manuscript that has been accepted for publication. As a service to our customers we are providing this early version of the manuscript. The manuscript will undergo copyediting, typesetting, and review of the resulting proof before it is published in its final form. Please note that during the production process errors may be discovered which could affect the content, and all legal disclaimers that apply to the journal pertain.

1
2
3
4 **IDENTIFICATION OF SPECIFIC SOURCES OF**
5 **AIRBORNE PARTICLES EMITTED FROM**
6 **WITHIN A COMPLEX INDUSTRIAL**
7 **(STEELWORKS) SITE**
8
9

10 **D.C.S. Beddows and Roy M. Harrison*†,**

11
12 **National Centre for Atmospheric Science**
13 **School of Geography, Earth and Environmental Sciences**
14 **University of Birmingham**
15 **Edgbaston, Birmingham B15 2TT**
16 **United Kingdom**
17
18
19
20

* To whom correspondence should be addressed.

Tele: +44 121 414 3494; Fax: +44 121 414 3708; Email: r.m.harrison@bham.ac.uk

† Also at: Department of Environmental Sciences / Center of Excellence in Environmental Studies, King Abdulaziz University, PO Box 80203, Jeddah, 21589, Saudi Arabia

21 **ABSTRACT**

22 A case study is provided of the development and application of methods to identify and
23 quantify specific sources of emissions from within a large complex industrial site. Methods
24 include directional analysis of concentrations, chemical source tracers and correlations
25 with gaseous emissions. Extensive measurements of PM₁₀, PM_{2.5}, trace gases, particulate
26 elements and single particle mass spectra were made at sites around the Port Talbot
27 steelworks in 2012. By using wind direction data in conjunction with real-time or hourly-
28 average pollutant concentration measurements, it has been possible to locate areas within
29 the steelworks associated with enhanced pollutant emissions. Directional analysis
30 highlights the Slag Handling area of the works as the most substantial source of elevated
31 PM₁₀ concentrations during the measurement period. Chemical analyses of air sampled
32 from relevant wind directions is consistent with the anticipated composition of slags, as are
33 single particle mass spectra. Elevated concentrations of PM₁₀ are related to inverse
34 distance from the Slag Handling area, and concentrations increase with increased wind
35 speed, consistent with a wind-driven resuspension source. There also appears to be a
36 lesser source associated with Sinter Plant emissions affecting PM₁₀ concentrations at the
37 Fire Station monitoring site. The results are compared with a ME2 study using some of
38 the same data, and shown to give a clearer view of the location and characteristics of
39 emission sources, including fugitive dusts.

40

41 **Keywords:** PM₁₀; steelworks; Port Talbot; source identification; fugitive emissions

42

43 **1. INTRODUCTION**

44 The town of Port Talbot in South Wales has long been recognised as having some of the
45 highest PM₁₀ concentrations in the United Kingdom (AQEG, 2011). Earlier source
46 apportionment studies have shown the large integrated steelworks operating within the
47 town to be an important contributor to elevated PM₁₀ levels (Taiwo et al., 2014a,b,c).
48 Hayes and Chatterton (2009) analysed PM₁₀ data from Port Talbot and suggested that
49 exceedences of the 24-hour PM₁₀ Limit Value (50 µg m⁻³) may be caused by a range of
50 sources and conditions. It was concluded that the main sources contributing to elevated
51 PM₁₀ were not from the blast furnaces and sinter plant stack, but rather due to wind-raised
52 dust from the blending plant or from the most likely potential source 'activities' on the
53 steelworks site listed as: Cambrian stone granulation; metal plating pits; furnace slag pits;
54 multiserv briquetting; multiserv steel slag solidification/demetalling/cutting; multiserv
55 scarfing activities; hot and cold mills; steel plant; demetalled BOS slag storage; furnace
56 slag storage and crushing. This agrees also with the findings of Guinot et al (2016) who
57 suggested - following their UV LIDAR study over a large integrated steel works in Spain -
58 that air quality management of steelworks needs to focus on controlling large and coarse
59 particle emissions, especially from open sources. Using positive matrix factorization, they
60 identified mineral dust being predominant in all size fractions, with the steelworks being a
61 clear source of carbonaceous species, and resulting in production of secondary inorganic
62 aerosols. In particular, stack emissions were identified as a major contributor of fine
63 particles, while open sources dominated the emissions of TSP, yielding up to 80% of
64 particles larger than PM₁₀. UV lidar provided 2D maps of aerosols in real time, with an
65 ability to detect PM emissions and to visualize complex plumes. For the Port Talbot
66 Steelworks, Taiwo et al. (2014a) attributed 23% of PM₁₀ mass measured off-site to
67 steelworks emissions from: blast furnaces (BF); basic oxygen furnace steelmaking plant

68 (BOS); and sinter unit, with the blast furnaces considered as the major contributor
69 accounting for one-fifth of the PM₁₀ mass. Coking and secondary aerosol accounted for
70 22% and traffic, marine and background aerosol accounted for 16%, 28% and 11% of the
71 PM₁₀ mass respectively. In addition, particle number concentration measurements by
72 Taiwo et al. (2014c) showed that local emissions, probably from road traffic, dominated the
73 smaller size bins (0.3–0.5 µm), while steelworks emissions dominated the range 0.5–15
74 µm, and for particles >15 µm marine aerosol appeared dominant.

75

76 Key trace elements attributed to the iron and steel industry include Cd, Cr, Cu, Hg, Ni, Se,
77 V, and Zn, and analyses of airborne PM close to steel plants have shown that Fe, Mn, Zn,
78 Pb, Cd and K are associated with emissions from the steel and iron plants (Kfoury et al.,
79 2016; Gladtko et al, 2009). Kfoury et al. 2016 applied a constrained weighted-non-
80 negative matrix factorisation model to PM_{2.5} composition data collected in Dunkerque,
81 Northern France in the vicinity of a steelworks. They identified 11 source profiles with
82 various contributions; 8 were characteristics of coastal urban background site profiles and
83 3 were related to the steelmaking activities. Between them, secondary nitrates, secondary
84 sulfates and combustion profiles give the highest contributions and account for 93% of the
85 PM_{2.5} concentration. The steelwork facilities contributed about 2% of the total PM_{2.5}
86 concentration and appeared to be the main source of Cr, Cu, Fe, Mn and Zn. Gladtko et al
87 (2009) measured PM₁₀ at four sampling sites in northern Duisburg; an area where iron and
88 steel producing industry is concentrated. They showed calcium, iron and zinc measured at
89 two sites close to the industrial area and information about the urban background aerosol
90 was sufficient to calculate the PM₁₀ contribution of the main single plants.

91

92 Focussing on specific sources, Hleis et al (2013) measured emissions directly from
93 sources within a steelwork in Northern France using particle size distribution, chemical
94 analysis, XRD, SEM-EDX and TGA/DTA. Samples collected from the sinter stack showed
95 high levels of K and Cl^- , followed by Fe, NH_4^+ , Ca, Na and Pb. Conversely dust samples
96 taken from the sinter cake discharge zone showed higher amounts of Fe, Ca and Al, and
97 lower amounts of K, Cl^- , Na and Pb. Dust samples collected from the blast furnace (BF)
98 and steelmaking cast house were distinguished from each other based on the higher
99 levels of Fe (hematite and magnetite) and lower levels of Ca, Zn and C (graphite) found in
100 BF dust. High levels of Ca and Fe were found in samples taken from the desulfurization
101 slag processing area. Microscopic analysis of individual particles has also identified
102 individual Fe-rich particles close to steel plants, e.g. Moreno et al. (2004) identified iron
103 spherules in both fine and coarse PM fractions at the steelworks in Port Talbot, South
104 Wales; Ebert et al. (2012) observed a significant fraction of individual iron oxides and iron
105 mixtures in airborne PM near a steel industry in Duisburg, Rhine-Ruhr area, Germany.

106

107 Apart from the primary particulate pollutants discussed above, industries are also known
108 for emission of gaseous pollutants such as carbon dioxide (CO_2), carbon monoxide (CO),
109 sulphur dioxide (SO_2), nitrogen oxides (NO_x) and hydrogen gas (H_2), and volatile organic
110 compounds (Tsai et al., 2008; Johansson and Soderstrom, 2011). Some of these gaseous
111 pollutants can be transformed into secondary aerosols which are commonly detected in
112 the atmosphere.

113

114 Although earlier studies have thrown useful light on the specific sources of particulate
115 matter from within the South Wales steelworks site, this study was designed to provide
116 more specific information on the emissions, which could inform mitigation strategies. It

117 provides a case study example of how a well-designed measurement programme can
118 provide the data needed to develop cost-effective control options by identifying key
119 sources of emission.

120

121 1.1 The Port Talbot Steelworks

122 The steelworks is sited on an area of $\sim 28\text{km}^2$ with a working area of $\sim 8\text{km}^2$. There are
123 $\sim 50\text{km}$ of roads (many unsurfaced), $\sim 100\text{km}$ of railway and approximately 25,000 vehicle
124 movements per day (Environment Agency Wales, 2009). Figure 1 presents a map of the
125 Port Talbot steelworks and shows the locations of the different processes and the
126 potential sources of particulate emissions which can be described as follows, according to
127 Laxen et al. (2010):

- 128 • Stockyards (green and grey): Most of the raw materials of coal, coke and iron-bearing
129 ores are imported through the deep water harbour and stored in one of the two main
130 stockyards (ore to the north of the site and coal to the south). Raw materials including
131 iron ores (FeO , Fe_2O_3 , Fe_3O_4), limestone (CaCO_3) and dolomite ($\text{CaMg}(\text{CO}_3)_2$) are
132 used in a blast furnace (BF) once prepared within the sintering step, while lime (CaO)
133 and fluorspar (CaF_2) are used in a BOS plant (Machemer, 2004). Fugitive dust from
134 this area is expected to have components including Fe, Ca, Mg and Mn (Dall'Osto et
135 al., 2012a).
- 136 • Coke Ovens (grey): Coal is carbonised to coke in a series of heated ovens with
137 minimal air. Coals of differing properties are blended to form a coke with the required
138 properties needed for the blast furnace. The heating process drives off volatiles and
139 the coke is quenched and transferred by lorry (along Site Roads SR1-4 highlighted in
140 the figure by red, amber and green) to the blast furnace. CO_2 , SO_2 , NO_x and soot

- 141 (particulate matter) are the main emission components. In the coke-making process,
142 major elements observed by Tsai et al. (2007) in the emissions included S and Na.
- 143 • Sinter Plant (brown): Raw materials are blended in long beds and the sintering
144 process produces a fused and partially reduced form of iron that can be used to make
145 molten iron more efficiently. As a result, emission components of KCl, Fe, Pb, Zn and
146 Mn are expected. KCl was also identified by Hleis et al., 2013 as a particulate
147 dominating the emissions from the sintering process stack. Tsai et al. (2007)
148 suggested that K and Pb which contribute a significant percentage (15 and 2%) to the
149 total observed particle mass, are associated with the sintering process. Similarly,
150 Oravisjarvi et al. (2003) found that the sinter plant contributed 96% and 95% of the
151 total measured concentrations of Pb and Cd at Rahee, Finland.
 - 152 • Blast Furnace (brown): Blast furnaces convert iron ores into molten iron using carbon,
153 in the form of coal and coke. The molten iron is captured in 'torpedoes' (cylindrical rail
154 cars) and the slag is either granulated (used in cement) or run into pits to cool, and
155 subsequently crushed. Fe and Mn are components of the tapping process followed by
156 Ca, Al, Si, S during the slag processing. Gaseous emissions of CO₂, SO₂, NO_x are
157 also expected from the stove heating
 - 158 • Basic Oxygen Steel-making (BOS) (pink): The 'torpedoes' transfer the molten iron to
159 the BOS plant where it is converted to steel. This process produces desulph slag
160 which is crushed. Fe, Zn, Pb and Mn are expected components. (Dall'Osto et al, 2008)
 - 161 • Slag Handling Area SHA (yellow and blue): Slag from the BOS process is stored in
162 pits and either reprocessed to extract residual metal and subsequently crushed (steel
163 slag) or treated as waste. These areas are labelled SHA and encompass the following
164 activities: furnace slag storage and crushing; Steel Slag Solidification, demetalling and
165 cutting and demetalling BOS slag and storage.

- 166 • Hot and Cold Mills (pink): Steel slabs are heated and rolled into a long thin coil of
167 metal. This is an energy intensive process. The hot forming process showed high
168 abundance of S, Fe, Na and Ca (Tsai et al., 2007). The study of Machemer (2004)
169 showed elevated concentration of Fe, Al, Si, S and Zn at sections in the vicinity of both
170 BOS and BF.
- 171 • Power Plants (light blue): Producing steel is very energy intensive both in electricity
172 and steam. Waste gases from the Coke Ovens and Blast Furnace are used as fuels.
- 173 • Site Roads SR1-6 (red,/amber/green). As to be expected, there is a network of roads
174 on the site, some made and unmade, and despite mitigation strategies such as
175 surface wetting and wheel washing, the regular usage of these roads by HGVs will
176 lead to resuspension of dust. The roads with substantial traffic are coloured, green,
177 orange and red in Figure 1.

178

179 2. METHOD

180 2.1 Measurement Sites

181 Port Talbot steelworks has eight council operated air quality monitoring sites positioned
182 around the North and North East boundary of the Steelworks (see Table 1,
183 www.welshairquality.co.uk). *Margam Fire Station* is the main monitoring site which is part
184 of the DEFRA Automatic Urban and Rural Network (AURN) network. The monitoring
185 station is within a self-contained, air-conditioned housing located within the grounds of a
186 fire station and measures the main particulate and gaseous metrics. The nearest road is
187 approximately 10 metres from the station and is an entrance to the steelworks. The
188 nearest main road is the A48 or Commercial Road. It is a 30 mph road approximately 115
189 metres from the station with 10,000 vehicles per day (2012) comprising 82% cars; 11.5%
190 Light Goods Vehicles LGVs; 3% Heavy Goods Vehicles HGV and 1.5% commercial

191 Passenger Carrying Vehicles PCVs. The M4 motorway is approximately 350 metres to the
192 NW with an annual average daily flow of 71,000 vehicles per day (averaged from 2014 to
193 2016 from Junction 39 to Junction 40 at Taibach). Of this 77.5 % are cars; 14.7 % LGV;
194 and 7.2 % HGV with the remaining 0.6 % made up of Two Wheeled Motor Vehicles
195 (TWMV) and PCV. The M4 is has 70 mph limit but as the road winds around Port Talbot a
196 50 mph speed limit is enforced by average speed cameras. The surrounding area is open
197 land associated with the steelworks and residential dwellings with a population of roughly
198 140,000 within the Neath-Port Talbot area. This equates to 317 people/km² compared to
199 632 and 2467 people/km² in Swansea and Cardiff respectively. Twll-yn-y-Wall, Talbot and
200 Theodore Road sites are roadside sites and only Twll-yn-y-Wall was included in this study
201 due to its closer proximity to the steelworks. Even though both the Talbot road and Twll-
202 yn-y-Wall sites are on the busy A48, Twll-yn-y-Wall Park is in a more open area compared
203 to the Talbot road site which could be considered a mini-street canyon. The Theodore
204 Road site is on a back street of Port Talbot and further away from the steelworks but much
205 closer to the M4. The other steel-work perimeter sites included the *Prince Street* site which
206 is within the open grounds of a quiet water pumping station. It is located next to the main
207 Swansea to London Paddington railway line on the side which is furthest from the
208 steelworks. This site is positioned the closest to the blast furnaces of the steelworks.
209 *Dyffryn School* (DS) is most Southerly site, exposed to emission from the mid section of
210 the steelworks with the closest source being the rolling mills. The site is next to the school
211 buildings but has a clear line of site - across playing fields and then over residential roof
212 tops - of the steelworks. Like Theodore Road, the DS site is close to the M4. Before the
213 opening (after this study) of the Port Talbot Distribution Road (PDR, designed to relieve
214 pressure on the M4 from local traffic) the *Docks* site was situated on a back road and was
215 described as an urban background site situated in an expanse. Although described as an

216 urban industrial site, the *Little Warren* site is situated on the the Southern tip of the
217 residential areas of Sandfields and Aberafan and is alongside a footpath running along the
218 mouth of the river Afan and Port Talbot Docks area. The closest source within the
219 steelworks to the LW site is from the stock yards. Furthermore, on the South side of the
220 estuary and on the coast is a break-water area where ships supplying the steelworks are
221 unloaded. All meteorological data was collected from the Mumbles Head Observatory in
222 Swansea (Met Office, 2012). It is positioned on a jut of land reaching out from the
223 Southern coast of the Gower Peninsular into the Bristol Channel and Swansea Bay. It is
224 roughly at a 10 km distance perpendicular to the coast running alongside Port Talbot
225 steelworks.

226

227 **2.2 Measurements**

228 Each of the 8 sites (Table 1) collected measurements of PM_{10} around the site as part of
229 the continuous monitoring programme carried out by Neath-Port Talbot Council. The
230 monitoring site at Margam, FS is part of the national Automatic Urban and Rural Network
231 (AURN) and in addition to PM_{10} , collected $PM_{2.5}$, O_3 , SO_2 , CO , NO_x , NO , NO_2 and
232 meteorological (met) data. The met data comprised wind direction, wind speed,
233 temperature, pressure, relative humidity and rainfall data. It was also at the FS that, our
234 main lab was deployed to collect campaign data in April and May of 2012. The instruments
235 deployed (Table 2) were used to collect chemical and physical data. Partisol-Plus
236 dichotomous sequential samplers (Thermo Scientific, Model 2025)) and Digitel high-
237 volume samplers (model DHA-80 Digitel Elektronik GA, Hagnau, Switzerland) were used
238 to collect daily $PM_{2.5}$ and PM_{10} filters for laboratory measurement of cations/anions/EC/OC
239 (Cl^- , NO_3^- , $nss-SO_4^{2-}$, Na^+ , NH_4^+ , K^+ , Mg^{2+} , Ca^{2+} , Al, V, Cr, Mn, Fe, Ni, Cu, Zn, Cd, Sb, Ba,
240 Pb, EC and OC, see Taiwo et al 2014a for more details). The Partisol used 47 mm

241 diameter, PTFE filters whereas the Digitel was loaded with quartz filters. Partisols were
242 also used to collect filters at the LW, PS and the LW sites. A Tecro Steaker sampler was
243 used to collect hourly PM_{fine} and PM_{coarse} filter measurements, measured off line for
244 elements (Na; Mg; Al; Si; S; Cl; K; Ca; Ti; Cr; Mn; Fe; Ni; Cu; Zn; Br; Sr; Pb) using PIXE
245 analysis (Lucarelli et al., 2011). A second Streaker sampler was also operated
246 concurrently at the LW site. We also collected BC data using a 7 wavelength Magee AE31
247 Aethalometer, single particle mass spectra using a TSI 3800 ATOFMS and particle
248 number data using a Grimm 1.108 particle spectrometer (Taiwo et al., 2014c).

249

250 With regards to meteorological data, for the study period considered by our 2012
251 campaign, data was only available from the Mumbles Head Observatory (MU).
252 Comparisons of this data set with the data measured at the Margam Fire Station (FS) site -
253 for an augmented period with measurements at the FS – showed a close relationship
254 between the wind directions with no offset. Modelled data was available at both the FS
255 and Little Warren (LW) and this also gave a close relationship but with an offset of 15-20°.
256 Similarly, there were linear correlations between the measured and modelled wind speeds
257 measured at the three sites. Although, the wind speeds modelled at the LW and FS were
258 96% and 40% of the values measured at the MU. Hence data from MU was used
259 throughout this analysis and was taken as representative of the conditions of the air
260 moving over the steelworks. However, it was recognised that the topography of the land
261 and buildings may affect the local movement of air around the site before arriving at the
262 monitoring sites resulting in anomalies within the data.

263

264 2.3 Data Analysis

265 Bipolar plots of the metrics versus wind direction and wind speed provide the foundation of
266 the first analysis carried out within this study. The bipolar plots were drawn using the Cran
267 R package, Openair (Carslaw and Ropkins, 2012). Hotspots are often identified in the
268 plots which show a range of wind directions and wind speeds where the measured metric
269 is elevated, thus identifying a source. The code used to create these was further
270 enhanced to add radial lines either sides of these hotspots. These marked a sector of
271 wind directions across which the measurement metric rose above a statistic (eg 85th, 90th,
272 95th percentile). In addition to the bipolar plots being useful to identify sources which
273 elevated the PM₁₀, bar plots were constructed from PM₁₀ measurements to show which
274 chemical constituents or ME2 source factors (marine; secondary; traffic; steel1, steel2,
275 steel3; sulphate, nitrate and background aerosol) derived from the constituents (Taiwo et
276 al 2014a) contributed most to the elevation of PM₁₀. ME-2 is a least squares program for
277 solving multi-linear problems. Specifically, it solves bilinear problems taking the form $X =$
278 $G \cdot F + E$. X is a matrix whose rows contain the hourly/daily measured chemical species
279 which is factorised into a combination of source factors F and their corresponding time
280 series G; matrix E is a remainder term. We were also able to provide supporting data from
281 ART2a cluster analysis of ATOFMS data and k-Means analysis of Grimm particle size
282 data.

283

284 3. RESULTS

285 The results presented are structured to further our understanding of the measurements of
286 common air pollutants made by the national monitoring (AURN) network around the
287 steelworks. The gas and PM measurements are considered and used to identify the most
288 likely source areas giving rise to the elevated concentrations of PM. This is then extended
289 using campaign data collected in 2012 at the Little Warren and Fire Station sites. In this,

290 two stories unfold, one which points to the Slag Handling area of the site, and another
291 which points towards the steel making processes.

292

293 3.1 Gases

294 At the Margam Fire Station AURN site, gaseous and particulate metrics are measured
295 continuously and include: NO; NO₂; NO_x; O₃; SO₂; CO; PM_{2.5} and PM₁₀. When the
296 average mass concentrations of the AURN gases are banded according to four ranges of
297 PM₁₀ (3-19; 19-35; 35-56; and 56-141 µg/m³) and then plotted, NO, NO₂ and NO_x are
298 observed to rise with PM₁₀ up to a PM₁₀ concentration of 50 µg/m³ (Table S1). O₃ shows
299 no trend with PM₁₀ but SO₂ and CO continue to rise with PM₁₀ above 50 µg/m³ suggesting
300 that the sources associated with the higher PM₁₀ concentrations are also linked to SO₂ and
301 CO emissions. Similarly for the meteorological data (Table S2), higher PM₁₀ values are
302 more likely for higher wind speeds and for wind directions between 186 and 227°, which
303 are directions in line with the northern and southern boundary of the Slag Handling area
304 (labelled as SHA in Figure 1). Although a general increase in PM₁₀ with wind speed
305 suggests a windblown dust source, 'hot-spots' within the wind roses have been observed
306 within this sector which suggests an influence of process sources (e.g. Steel and Slab,
307 Ironmaking).

308

309 Road activity and fugitive dusts from material handling and storage are expected to make a
310 significant contribution to PM alongside Stack and Diffuse emissions from plant processes,
311 e.g. Sinter and BOS plant (Tata Steel, personal communication). When viewed from the
312 AURN site at Margam Fire Station, any PM contribution due to the road activity through
313 the Slag Handling Area is in the shadow of the region of the Blast Furnaces which will also

314 make a contribution in this wind sector. The Slag Handling Area represents the combined
315 area used to process the slag generated from iron and steel making.

316

317 The pollution roses (for NO, NO_x and CO) in Figure S1 all show a hot spot for wind
318 directions (209-232°) from the south west of the monitoring station and for elevated wind
319 speeds between 7 and 18 m/s. NO_x and CO appear most probably to be a combination of
320 the emissions from the Sinter Plant and Blast Furnaces. However, this angle of wind
321 direction encompasses not only the Sinter Plant and Blast Furnaces, it also encompasses
322 the road emission sources passing along the coastal roads (orange SR1 and red SR2) and
323 through the Slag Handling Area. It is referred to as Meteorology Case 1. Likewise, PM_{2.5},
324 PM₁₀ and SO₂, (Figure S2) are elevated in concentration for wind speeds between 7 and
325 18 m/s, albeit for a similar range of wind directions rotated slightly clockwise to include
326 more of the emissions from the Sinter Stock source and their roads (green SR4)– referred
327 to as Meteorology Case 2. Also, within this sector area around the blast furnace are three
328 areas marked in yellow. These, from West to East include: the Coal Injection Plant;
329 Granulation Activities and the Furnace Slag Pits. SO₂ is more likely to be an emission
330 from the Sinter Plant accompanied by fugitive dusts from within the vicinity, e.g. from the
331 conveying of raw materials. It might also be expected that PM arises from raw materials
332 containing heavy metals associated with the sintering process,(e.g. Zn, Pb and Cd),
333 where some may be volatilised directly or converted into volatile compounds, e.g.
334 chlorides, seen in the ATOFMS cluster 13 K-Cl, with possible Cd and Pb peaks (at m/z
335 110-114 and 208 respectively; Figure S3), and occurs in the flue gas. Non-volatile and
336 volatile PM_{2.5} are measured using the TEOM FDMS and the non-volatile fraction makes up
337 most of the PM_{2.5} and has a similar windrose. The volatile fraction is different, in that

338 points towards the SSE, possibly influenced by regional transport of semi-volatile
339 ammonium nitrate.

340

341 **3.2 Particulate matter (PM) mass**

342 Figure 2 shows concurrent PM_{10} measurements at the LW and the FS sites constraining
343 the emission to high speed winds (10-15 m/s) passing over the Blast Furnaces, Sinter
344 Plant, Slag Handling area and Ore Stock Yard. Comparing the two PM_{10} wind roses for
345 the Little Warren and Margam Fire Station sites, the maximum hourly PM_{10} value
346 measured was 35 and 210 $\mu\text{g}/\text{m}^3$ respectively. The larger spread of wind directions
347 associated with high concentrations at the LW compared to the FS site is best explained
348 by a line source which is perpendicular to the line of sight to LW and in line with the FS
349 site. When the wind blows across the line source towards LW, the PM_{10} rises to a
350 maximum of 35 $\mu\text{g}/\text{m}^3$ at any one point along the line source and arriving at the LW site
351 within the acceptance angle α . However, when the wind blows along the line source, there
352 is approximately a six-fold increase in concentration of PM_{10} to in excess of 210 $\mu\text{g}/\text{m}^3$
353 over smaller acceptance angle β . The two PM_{10} wind roses constrain the emission area
354 to the upper part of the Slag Handling area, the Sinter Plant and the more northerly Blast
355 Furnace. The non-volatile PM_{10} shows a similar directional association to the PM_{10} wind
356 rose but the volatile PM_{10} emissions are in the direction of the mill and off-site sources and
357 like volatile $PM_{2.5}$ make a small contribution to the PM_{10} of 5 $\mu\text{g}/\text{m}^3$.

358

359 The source area is constrained further to just the Slag Handling area when considering
360 PM_{10} measurements from the Docks and Dyffryn School (Figure 3) and if a line source is
361 suspected as being responsible for the elevated emission then one of the roads passing
362 through the Slag Handling Area is a good candidate. Figure 3 superimposes onto the map

363 the PM_{10} wind roses calculated for the six sites considered and for each wind rose two
364 radial lines are marked where the PM_{10} concentration is at the 90 percentile ($PM_{10} = 38$
365 $\mu\text{g}/\text{m}^3$ at FS). Bipolar plots for Talbot Road and Theodore Road are given in Figure S4.
366 These were omitted from the analysis due to their locations, i.e. being within a mini canyon
367 and close proximity to the M4 motorway respectively. However, in spite of this, a
368 retrospective view of the data collected at these two sites supports the conclusions derived
369 from the other Port Talbot sites. Using the pairs of radial lines for each site, two extreme
370 areas can be marked out shown by the black and grey boundaries. The grey and black
371 boundaries represent the minimum and maximum source area, respectively, for which the
372 PM_{10} concentration is over the 90 percentile. Addition of the PM_{10} wind roses collected at
373 Prince Street and Twll-yn-y-Wal Park to this plot complements this observation and the
374 aerial view (<https://www.google.co.uk/maps/@51.571154,-3.78268,16z>) underneath the
375 black boundary clearly shows a grey dusty handling area which is in sharp contrast to the
376 black and brown rust dust areas around other operations on site. This is a different result
377 to that presented in the AQEG (2011) report "Understanding PM_{10} in Port Talbot", which
378 circles the area east of the Slag Handling area which includes: Blast Furnaces and Slab
379 Yards.

380

381 To visualise the magnitude of the PM_{10} values in these pollution roses, Figure 4 shows the
382 values of the maximum PM_{10} values for these sites. For all of the sites, over half of the
383 time, the PM_{10} is below $20 \mu\text{g}/\text{m}^3$ (cf 2012 annual mean of $18 \mu\text{g}/\text{m}^3$ at both Swansea
384 Road in Swansea (*lat* = $51^{\circ},37',57.706''\text{N}$, *long* = $3^{\circ},56',50.546''\text{W}$) and Cardiff Central (*lat*
385 = $51^{\circ},28',54.408''$, *long* = $3^{\circ},10',34.500''\text{W}$)). But at the FS and PS sites, there is a notable
386 high percentage of occurrence of PM_{10} values above $20 \mu\text{g}/\text{m}^3$. The PS site records the
387 highest PM_{10} values and the Docks the lowest. The magnitudes measured at the different

388 sites can be understood by considering the distance between these sites and the various
389 sources. In particular, there is a distinct PM_{10} -distance relationship when considering the
390 area in and around the Slag Handling Area (see Figure 5a). The mean PM_{10} value
391 correlates with the inverse distance to the receptor sites from the centre of the Slag
392 Handling Area. This relationship remains when considering the maximum PM_{10} values as
393 a function of inverse distance from the Slag Handling area. The maximum values
394 measured at Dyffryn School (DS) and Twll-yn-y-Wal (Twll) do not fit this linear trend but
395 the measurements are brought into line when considering the 90th percentile (Figure 5b,c).

396

397 When considering the wind roses at the LW and FS expressed as Conditional Probability
398 Functions (Uria-Tellaetxe and Carslaw, 2014), the contribution of the steelworks source
399 become significant for the 75-100th percentile of data (Figure 6a). This corresponds to
400 PM_{10} values between 23-99 and 27-210 $\mu g/m^3$ for the LW and FS sites respectively. For
401 percentile ranges below 75% the CPF wind roses point away from the steelworks (Figure
402 6b). This gives a clear indication that for the campaign period, a source within the area
403 bounded by the bold line in Figure 6a was responsible for the high PM_{10} values. It is also
404 worth mentioning that at the LW site, the main source detected is from the West (from sea
405 spray) due to its close proximity to the coast, and in comparison, there is less than 60 %
406 conditional probability that the elevated PM_{10} at the LW is from the direction of the
407 steelworks. A comparable strong Westerly source from the sea is not observed at the FS.

408

409 **3.2.1 AURN data (PM_{10}) corrected for upwind background**

410 Further results are obtained by estimating the increment due to the steelworks which can
411 be considered by measuring the difference between the foreground (Downwind) and
412 background (Upwind) sites (Figure S5 and S6). Two cases are presented. In Cases 1

413 and 2, the PM_{10} measurements from the LW and FS sites are selected by wind direction
414 $162-270^\circ$ and $100-152^\circ$ respectively and each set is averaged. In Case 1, the wind
415 direction is from the sea passing over the steelworks. For this, the LW is the Upwind and
416 the FS is the Downwind site. For Case 2, the wind direction is along the coast and wind
417 directions are chosen such that the LW measures the increment above the FS which
418 pertains to the steelworks. A clear increase in PM_{10} ($11 \mu\text{g}/\text{m}^3$) and Non-Volatile PM_{10} can
419 be seen for case 1 (Figure S5, where only PM_{10} was measured at LW). There is no
420 change in Volatile PM_{10} suggesting that the rise in PM_{10} is more likely from wind-blown
421 dust. This same increment is observed for Case 2 where LW is downwind of the FS site
422 (see Figure S7) together with an effect due to the traffic along the M4 motorway raising
423 NO_x and $PM_{2.5}$ to higher values than those seen in Case 1.

424

425 3.3 Chemical Measurements

426 3.3.1 Streaker/PIXE Data

427 The increment in PM can be further examined using the chemical composition measured
428 using hourly Streaker/PIXE measurements (Figure S7, S8, S9 and S10). For Case 1, the
429 wind blows from the sea, across the Slag Handling area, Sinter Plant and Blast Furnaces
430 to the Fire Station site. Comparing the Streaker/PIXE data measured at the Fire Station
431 with the Streaker/PIXE data measured at Little Warren, an increase in all fine and coarse
432 elements is seen (except for fine Na and Cl). There is a notable increase in S, Ca and Fe
433 in both size fractions and Na, Cl, Mg, Al and Si in just the coarse fraction. For Case 2, the
434 same comparison between downwind and upwind Streaker/PIXE data, is not as clear-cut.
435 An elevation in fine Na, Ca, K, S and Fe and only coarse Ca and Fe is seen with a
436 marginal increase in Si. When this analysis is repeated for wind directions passing over
437 the Slag Handling area (Figure S10), an enhancement is seen in fine Ca, Fe, K, Mn and

438 Zn and coarse Al, S, Ca, Fe and Si for Case 1 (when the wind blows along the length of
439 the source) and in fine Na, Mg, Al, S, Cl, K, Ca, Fe and Sn and coarse Na, Mg, Al, S, Cl,
440 Ca, Fe and Si in Case 2 (when the wind blows across the source). For the purpose of this
441 comparison, the LW data have been scaled by a factor of 2.1 to allow for enhanced
442 dilution (compared to FS) during transport from the Slag Handling Area (based on findings
443 illustrated in Figure 5). Fine K, Ca, Fe and Zn are all enhanced for both Case 1 and 2.
444 However, Ca and in particular Fe, are considerably enhanced for Case 1. In comparison
445 with the work of Taiwo et al. (2014b) this is characteristic of the Blast Furnace Factor (see
446 below, ME2 section). For the coarse measurements, the main components that are
447 enhanced are S (in Case 1), Ca, Si and Fe. This is consistent with emissions from a line
448 source passing through the Slag Handling area whose main components are enhanced
449 Fe, Ca and Si.

450

451 The contribution of each of these elements for various PM_{10} concentration ranges is shown
452 in Figure 7a. Fe is clearly a key constituent elevating the PM_{10} followed by Ca and S. The
453 contribution of these elements to the PM_{10} rises from less than 10% to 50% for the 56-141
454 $\mu\text{g}/\text{m}^3$ range. There are also significant contributions from Na, Mg and Cl. Figure 7b
455 shows the same result but for wind speed suggesting that during the campaign the source
456 is not from a process source but from a wind driven source, e.g. surface dust on a road.
457 The contribution of Fe and Ca only increases for wind speeds above 6 m/s.

458

459 3.3.2 ME2 Results

460 Considering the ME2 source apportionment results derived from the Streaker/PIXE data
461 by Taiwo et al. (2014a) (Figure 8), all factors contribute to the elevation of PM_{10} , namely,
462 Steel 1 and Steel 3, followed by Sintering, Steel 2, Marine and Background Aerosol.

463 Again, all wind-driven sources are shown in Figure 8b Steel 1, 2 and 3 are associated with
464 Blast Furnace, Coking Process and BOS plant respectively. The Steel 1 source is
465 characterised by high concentrations of both Ca and Fe; Steel 2 is characterised by high
466 levels of Fe, Ca, Na and Zn; Steel 3 is high in sulphur; and Steel 4 has high concentrations
467 of Ca, Si and Al. Steel 1 and Steel 3 make the highest contribution to the elevation of
468 PM_{10} and have time series with a high correlation to PM_{10} mass (0.7 compared to less
469 than 0.13 for the other factors) indicating that they are possibly from the same source or
470 area of wind blow dust, comprised largely of Fe, Ca and S.

471

472 3.3.3 Effect of Rainfall

473 If windblown dust is suspected as being responsible for the elevation of PM_{10} , then
474 changes in the PM according to rainfall might be expected. Figures S11a and S11b show
475 how the PM_{10} values varied for all 8 Port Talbot sites. Average values fall with increased
476 rainfall as a general trend. The difference in the Streaker/PIXE data measured on a dry
477 day compared to a wet day again consistently shows an elevation of Ca and Fe in the fine
478 and coarse modes on dry days. Coarse sea salt elements (Na, Mg and Cl) are all
479 enhanced on a dry day together with Al, Ca, K and Fe (Figure S11d). Fine Ca and Fe are
480 also enhanced on a dry day together with elements Mg, Al, S, Cl, K, Ti, Mn, Zn and Pb
481 (Figure S11c).

482

483 3.3.4 Correlation with AURN Trace Gases

484 The correlation of these Streaker/PIXE measurements with the gaseous pollutants
485 measured at FS site has also been considered. Table S3 shows the correlation coefficient
486 calculated between the Streaker/PIXE increments and the gas measurements collected at
487 the Fire Station site. There is no significant correlation for meteorology Case 2, but for

488 Case 1 we see strong correlations between: SO₂ and fine K, Al, Fe, Pb, Mn, Se and S;
489 SO₂ and coarse K, Ca, Al, Fe, Cr, Pb, Ti, Mn and S. Likewise, there are strong
490 correlations between CO and fine Mg, K, Ca, Al, Fe, Zn, Pb, Mn, Se and S; and CO and
491 coarse K; Ca; Al; Fe, Zn, Cr, Ti, Mn and S. Figure S12 plots these relationships, showing
492 the strongest relationships between fine and coarse Fe, Ca and S with SO₂ and CO.
493 These results are presented graphically for SO₂ and CO in the columns of the correlation
494 plots in Figure S13. In these plots, high correlation between SO₂ and fine K, Pb, S and
495 Se; CO and fine Al, Ca, Cl, Fe, Mn, Pb, S, Se, Ti and Zn; SO₂ and coarse Al, Cl, Fe, K,
496 Mg, Mn, Na, Pb, S and Ti; and CO and coarse Ca, Cr, K, Mg, Mn, Na, Ti and Zn are
497 observed. Also, natural groupings amongst the fine and coarse Streaker/PIXE elements
498 are seen. For example, in the fine fraction, a grouping of fine Fe, Al, Ca, Mn, S, Se and Ti
499 and coarse Fe, Ca, Cl, Cr, K, Mg, Mn, Pb, S and Ti are seen. Interestingly, Ni and Cr have
500 the lowest or negative correlations. It seems likely that the elements associated with fine
501 particles may arise from the same source of process emissions as the SO₂ and CO
502 (presumably the sinter plant and blast furnaces) while the coarse fraction metals more
503 probably arise from the area in and around the Slag Handling area, which is on the same
504 wind sector from the sampler.

505

506 3.5 ATOFMS

507 There have been a number of earlier deployments of the Aerosol Time-of-Flight Mass
508 Spectrometer (ATOFMS) at Port Talbot, reporting measurements of metallic (Dall'Osto et
509 al., 2008a) and non-metallic (Dall'Osto et al., 2012b) species, and the full range of
510 particles (Taiwo et al., 2014b).

511

512 Table 3 presents a summary of the results of the ART2a analysis of the ATOFMS mass
513 spectra collected during the four week campaign (details are in Taiwo et al., 2014b) at the
514 FS site. From this, a general background made up of the first main clusters 1-5 consisting
515 of regional nitrate, sulphate, sea salt and EC is seen. Not reflecting the mass detected,
516 these ATOFMS clusters account for ~80% of the number of detected particles. The
517 remaining 20% can be attributed to sources within and around Port Talbot and are
518 associated by polar plots with high counts for winds from the SW with high speed, i.e.
519 wind-blown sources, namely clusters 6, 7, 9, 13, 14 and 16 (Figures S3a and S3b).

520 The polar plots of clusters 6 and 7 point to several sources in the south of the site (similar
521 to Met. Case 2) and include the: Blast Furnaces; Slag Handling Areas (SHA 3-4); Metal
522 Plating pit; BOS plant; Coke Ovens and Site Roads (SR 1-4). The polar plots for clusters
523 9, 13 and 16 (Met. Case 1) include the: Power Plants; Blast Furnaces; Sinter Plant; Slag
524 Handling Areas (SHA 1-3); Metal Plating pit; Coke Ovens and Site Roads (SR 2-4 and 6).

525 Cluster 14 is peculiar in that it has a very narrow angle of occurrence and neatly
526 encompasses the Furnace Slag Pits. It had the chemical signature of Amines as a single
527 24 hour episode of particles with a 2.0 μm mode.

528 Clusters 9, 13 and 14 have wind roses which point towards the Blast Furnaces and Slag
529 Handling area whereas clusters 6 and 7 have wind roses which are more associated with
530 winds passing over the southern part of the steelworks (including Slab Yards 1 and 2 and
531 the Coal Stock Yard). The behaviour of these clusters suggests wind-blown dust but their
532 composition suggests a steel-making process. The wind roses of each of these clusters
533 point towards the same region of the Slag Handling areas marked in Figure 3. Cluster 9 is
534 interesting in that it has a road traffic signature and the wind rose points to an area
535 covering all of the Slag Handling region and Ore Stock Yard. In combination, clusters 13,
536 14 and 16 suggest a source with contributions from the following constituents: Na, K, Fe,

537 Cd, Pb, S, CN, Cl, NO₃, SO₄ and PO₃ all of which can be associated with Blast Furnace
538 and/or Sinter Plant emissions. Without at second ATOFMS operating at a second site
539 (such as the LW), or a library of ATOFMS data collected from each of the sources on site
540 to carry our a Discriminant Analysis, it is difficult to isolate sources. Hence, with ATOFMS
541 data, we can conclude the influence of two types of dust areas (to the SW and SSW of the
542 FS) and vehicle emissions encompassing the main site roads (SR 1-4).

543

544 **3.6 Physical Measurements**

545 **3.6.1 Overview of the Data**

546 Particle size distributions were measured during the campaign using a Grimm Dust
547 Monitor v1.108. This was operated at the Fire Station site and the average results are
548 presented in Figure 9. To differentiate between the steelworks (wind sector 270° through
549 0° to 140°) and background (wind sector 270° through 180° to 140°), two wind sectors
550 were considered (figure 9a). The number distribution (Figure 9b) was converted to volume
551 (dV/dLog(Dp)) and revealed four modes with modal diameters Dp = 0.3, 0.9, 2.0 and 5.0
552 µm. Furthermore, the modes centred at 2.0 µm and 5.0 µm can be seen to be elevated
553 when the wind sector includes the steelworks. Hence it can be concluded that this may be
554 the mode which is contributing to the elevation of PM₁₀ at the FS site. Figure 10a
555 considers the volume distributions for various PM₁₀ ranges from 0 to 61 µg/m³ and shows
556 that as PM₁₀ increases, the modes fitted at 2.2 and 4.5 µm both increase, the latter with a
557 slightly higher gradient. Figure 10b confirms that both the 2.2 and 4.5 µm modes
558 contribute to the elevation of PM₁₀ whereas the smaller modes in the distribution do not.

559

560 **3.6.2 K-Means Cluster Analysis**

561 A general overall picture of the particle volume size distribution spectra can be obtained by
562 analysing the hourly spectra using *k*-Means cluster analysis (see Beddows et al. (2009) for
563 methodology). This resulted in six clusters whose frequency is shown in Figure S14a.
564 The Cluster Proximity Diagram (Figure S14b) shows how the clusters are arranged
565 according to their similarity to each other; similar clusters are placed close to one another
566 whereas dissimilar clusters are placed far apart. Figure S15 shows the average particle
567 volume spectrum of each cluster together with the diurnal cycle of the cluster and the wind
568 rose associated with that cluster. The most frequent clusters are distinguished from each
569 other as being steelworks and background spectra. Cluster 1 and 2 have strong peaks at
570 2.5 μm compared to the 5.5 μm peak. Cluster 1 occurs during the day and for wind
571 directions passing over the Ore Yard, Slag Handling Plant, Sinter Plant and Blast
572 Furnaces. Cluster 2 is strongest for wind directions blown from inland and occurs mainly at
573 night. Clusters 5 and 6 do not have a clear diurnal pattern but are strongest for inland
574 winds passing over the M4 motorway which is probably reflected in the high mode below
575 0.5 μm . Clusters 3 and 4 are more interesting because they are both daytime clusters and
576 occur for wind directions passing over the Slag Handling area and Ore Yard respectively.
577 Both clusters have elevated modes at both 2.5 and 5.5 μm suggesting a characteristic of
578 the line source elevating PM_{10} .
579 The composition of these clusters can be derived using the Streaker data collected at the
580 LW and FS sites. Cluster 1 is associated with elevated Sea Salt (coarse Na, K, Mg and
581 Cl) but is also accompanied by a significant increment from dust (coarse Al and Ca) and
582 Fe and S in the fine and coarse mode (Figure S16). These same increments are not as
583 pronounced for the background cluster, cluster 2 and considering the different wind
584 directions, it is clear that S, Ca and Fe are higher when the wind blows across the site.
585 Small increments in Fe and Ca are observed for cluster 3 with significant increases in S

586 and BC but for a narrow wind sector passing over the Slag Handling area. There is also
587 an unexpectedly high measurement of Zn at LW, possibly from a wind direction blowing
588 across a source at the South of the site. Considering the wind rose, with its high speed
589 westerly winds, cluster 4 is a strong steelworks cluster and this is supported by the strong
590 enhancement of fine S, Ca, Fe and BC and coarse Mg, Al, S, K, Ca and Fe. Clusters 5
591 and 6 are interesting in that they show a very strong increment of sulphur in both the fine
592 and coarse ranges although considered to be a background cluster. This is probably
593 regional sulphate pollution due to long-range transport.

594

595 3.6.3 Contributions to PM₁₀

596 From the findings of this work, it can be seen that both process emissions and wind-blown
597 dusts are responsible for the elevation of PM₁₀. Using SO₂ as a marker of process
598 emissions and the sum of the Grimm size bins from 3 to 20 µm as a metric for
599 resuspended dust an estimation of the contribution of each to PM₁₀ can be assessed by
600 regressing PM₁₀ upon SO₂ and Dust all normalised to their maximum value. Equation 1
601 shows the result of this regression.

602

$$\frac{PM_{10}}{\max(PM_{10})} = 0.53 \times \frac{SO_2}{\max(SO_2)} + 0.41 \times \frac{\text{Dust}}{\max(\text{Dust})} + 0.043$$

603 This suggests that both process emissions and wind-blown dusts make a similar
604 contribution to the elevation of PM₁₀. In fact when regressing PM₁₀ against SO₂, NO_x, CO
605 and Dust, the regression factors are 0.44, 0.03, 0.1 and 0.40 confirming the major
606 contributors to PM₁₀ as a process or processes also emitting SO₂ and wind-blown dust.
607 The former probably include the blast furnaces and sinter plant.

608

609 4. CONCLUSIONS

610 Campaign data sets collected in April and May of 2012 around the Port Talbot steelworks
611 have been further analysed. Hayes and Chatterton (2009).concluded that the PM_{10}
612 exceedences within the Port Talbot conurbation were most likely to be from fugitive dusts
613 arising from within the steelworks. In particular, emissions from vehicular movement on
614 the roads on the site and emissions from the material storage and handling appeared to be
615 likely candidate sources. Our campaign data provide quantitative evidence in relation to
616 those sources

617

618 Considering the AURN gas data measured at the sites in Port Talbot, wind roses of the
619 trace gases measured at the FS site identify two source directions covering either the
620 Blast Furnaces and the whole of the Slag Handling area (NO , NO_x , O_3 and CO) or the
621 Sinter Plant and the more Northern parts of the Slag Handling area (SO_2 , $PM_{2.5}$, and
622 PM_{10}). It is the second case which includes wind directions yielding the higher PM
623 concentrations which are of interest in this work to understand the elevation of PM_{10} . Plots
624 showing the Streaker/PIXE data vs these trace gases show that Fe and Ca have a positive
625 dependence although not a significant correlation compared to other metrics.

626

627 When including receptor sites additional to the main AURN site at the FS, characteristics
628 of the source(s) of PM are observed. The maximum PM_{10} concentration measured at the
629 FS is six times higher than the maximum PM_{10} measured at Little Warren and this
630 difference can be accounted for by an inverse relationship between the PM_{10} value and the
631 distance between the centre of the Slag Handling area and receptor sites. Also there is a
632 large difference in the spread of wind directions for each site when PM_{10} concentrations
633 are highest (LW and FS) which can be explained by a line source passing perpendicular to
634 the LW site and toward the FS site. Inclusion of PM_{10} wind rose data collected at the Port

635 Talbot Docks, Prince Street, Twll-yn-Wall and Dyffryn School sites supports the conclusion
636 that a line source through the Slag Handling area is largely responsible for the elevation of
637 PM_{10} . Furthermore, when considering the PM_{10} wind rose in terms of conditional
638 probability at the LW and FS, it is clearly seen that elevations of PM_{10} above the upper
639 quartile of data (19 and 24 $\mu\text{g}/\text{m}^3$ for LW and FS respectively) are most likely to occur
640 when the wind blows from the coast and over the steelworks. If the PM_{10} is less than the
641 upper quartile of PM_{10} then it is most likely that the wind is blowing from the sampling sites
642 towards the steelworks. This is also consistent with a source on the steelworks site - most
643 likely a line source within the Slag Handling area – being largely responsible for the
644 elevation of PM_{10} in Port Talbot.

645

646 When dividing the data according to wind speed and PM_{10} concentration, an elevation of
647 PM_{10} for wind speeds above 6 m/s is observed. Considered as a moderate breeze, a wind
648 of 6 m/s will cause dust and loose paper to be raised off the ground and into the air. At
649 this wind speed, small waves on the sea will become larger and fairly frequently ‘white
650 horses’ giving rise to sea salt spray are observed. Using the Streaker/PIXE data, the
651 elevation of PM_{10} can be attributed in part to sea salt but is mainly associated with Fe and
652 Ca. We also see an increase in sulphur although it does not make a significant
653 contribution to the PM_{10} mass. The ME2 sources identified by Taiwo et al. (2014a), by
654 receptor modelling of the same data, point the responsibility for elevated PM_{10} towards
655 their Steel 1 and Steel 3 factors which were attributed to the Blast Furnaces and Coking
656 processes. These factors have a large association with Fe, Ca and S but are also linked
657 to Mg, Al, Si, Ti and Mn for the case of Steel 1 and Cu and Pb for Factor 4 implying that
658 they are more likely from a wind-blown dust arising within the area in and around the Slag
659 Handling area rather than a direct process emission. Again, the increase of PM_{10} with wind

660 speed is consistent with a resuspension source compared to a constant process source
661 which is more likely to decrease in concentration with increasing wind speed.
662 Furthermore, the PM_{10} data measured at the receptor site closest to the Slag Handling
663 area, and in line with a potential line source (i.e. at the FS), show a decrease in
664 concentration with increased rainfall. This provides further support for a resuspension
665 source because the same observation is not made at receptor sites furthest away from the
666 Slag Handling area and perpendicular to a potential line source. Differences between 'wet'
667 and 'dry' days at the FS site show an increase in coarse Na, Cl, Ca and Fe on the 'dry'
668 days. Similarly, fine Ca, Mg, Al, S, Cl and notably Fe increase on 'dry' days. Further
669 support for a wind-blown dust source can be derived from the particle size-volume spectra
670 measured at the FS where four modes are identified in the data, centred at 0.35, 0.89, 2.2
671 and 4.5 μm , and it is the latter two coarse modes which are correlated to PM_{10} mass.

672

673 Considering the coarse particle Streaker/PIXE data, Fe and Ca are highly correlated to Mg
674 and Mn which are characteristic of a stockyard fugitive dust but they are not as strongly
675 correlated to CO and SO₂ giving further confidence that the source is associated with
676 wind-blown dust rather than a process emission such as coking or power generation.
677 There are further strong correlations of Fe and Ca to Al and S which indicate a source
678 consistent with a wind-blown dust from the Slag Handling Area. There are also strong
679 correlations to Cr, Mg, Mn, and Ti. Fe also has its own additional strong correlation to Pb,
680 K and Cl which is characteristic of a Sinter Plant dust which may also be contributing to a
681 smaller extent to the elevation of PM_{10} . The absence of silicon within the PIXE analysis of
682 the Streaker data makes it difficult to explicitly link the chemical profile to a Slag Handling
683 process.

684

685 Analysis of the qualitative ATOFMS data (particles aerodynamic diameter < 3.5 μm)
686 collected at the Fire Station showed that the most frequently detected particles (by
687 number) were from background sources such as sea salt, regional sulphate, regional
688 nitrate and elemental carbon. Following these in magnitude were clusters of particles with
689 signals from PAHs, metals, phosphate, copper, chloride and sulphur which were all
690 attributable to the steelworks. Out of these clusters, those whose wind rose pointed
691 towards the Slag Handling area contained coarse Fe, Ca, Si, K, Cl, CN, phosphate and S,
692 elements expected to be characteristic of slag handling. There was also a 24 hour
693 episode from this wind direction which contained a 2.0 μm mode of amines. Also worth
694 noting was that PAH and Fe-PO₃ clusters were most associated with southerly wind
695 directions. As a postscript to the ATOFMS reanalysis, although ART2a cluster analysis
696 was used to find the most natural groups within the data, the full potential of this high
697 resolution data may not have been realised. The use of Discriminant Analysis to assign
698 the data collected during the campaign to source specific profiles derived by at-source
699 measurements, e.g. the Slag Handling area, Blast Furnaces, Sinter Plant, etc. may be
700 more fruitful using a nozzle inlet with a much higher upper size range.

701

702 A number of other studies have reported measurements of particulate pollution in the
703 vicinity of steelworks, located in northern France (Hleis et al, 2013) Kfoury et al, 2016),
704 southern France (Sylvestre et al, 2017), northern Spain (Ameida et al, 2015; Guinot et al,
705 2016) and northern Germany (Gladtkke et al, 2009). Both Sylvestre et al (2017) and
706 Kfoury et al (2016) focus upon the PM_{2.5} size fraction. As in our study, the steelworks
707 does not make a major contribution to this size fraction (about 2% in the case of Kfoury et
708 al, 2016), with metals being significant contributors to the emissions. Hleis et al (2013)
709 characterise the chemical profiles from different sources, and as noted above, these are

710 consistent with our own findings and assisted in identifying source areas. Both Almeida et
711 al (2015) and Gladtko et al (2009) found major contributions to PM_{10} from the blast
712 furnaces and sinter plant. In the former case, chemical profiles broadly similar to our own
713 were reported (Almeida et al, 2015), while in the latter, Ca, Fe and Zn were considered
714 sufficient to estimate PM_{10} contributions from the main plants. Our analysis provides a
715 more detailed characterisation, hence allowing differentiation between the sources, Guinot
716 et al (2016), differentiated between process (stack), fugitive and open sources emissions
717 by use of lidar and a PMF study based upon measurements of chemical composition. In
718 terms of contributions to TSP, open sources (40%) were the largest contributor, followed
719 by stack (18%) and fugitive (10%), on top of the regional pollution (32%). Open sources
720 described wind blown dusts, and the blast furnace slagging process was noted as a
721 particular source, consistent with our own observations.

722

723 In conclusion, the analysis presented shows that the steelworks is responsible for the
724 upper quartile of measured PM_{10} at the FS AURN site. PM_{10} wind roses locate the source
725 within the Slag Handling area and the varied range of wind directions over which PM_{10} is
726 high at the FS and LW sites suggest a line source. Furthermore, there is a strong
727 correlation between the upper 90 percentile of PM_{10} concentrations and the inverse
728 distance between all of the receptor sites around the steelworks and the centre of the Slag
729 Handling area. The particles are within the coarse mode of the volume distribution and
730 their elevation with increased wind speed and decrease with rainfall suggest that a wind-
731 blown dust rather than a process emission is responsible. The chemical composition
732 associated with the source has strong contributions from Fe and Ca which are
733 characteristic of a dust from the steelworks, and most likely the Slag Handling process.

734 There is also a contribution from particulate matter from a process also emitting sulphur
735 dioxide, probably the blast furnaces and/or sinter plant.

736

737 Prior to this study, the specific sources of particles within the steelworks had long been
738 unclear (AQEG, 2011), hence delaying fully effective control measures. The study shows
739 how it is necessary to apply a range of complementary methods to give a clear picture of
740 the emission sources, and that this complements and extends the insights gained from
741 application of the ME2 model.

742

743 **ACKNOWLEDGEMENTS**

744 The authors are grateful to the Welsh Government for funding the additional data analyses
745 reported in this paper.

REFERENCES

- 746
747
748 Almeida, S.M., Lage, J., Fernandez, B., Garcia, S., Reis, M.A., Chaves, P.C., 2015.
749 Chemical Characterisation of atmospheric particles, and source apportionment in the
750 vicinity of a steel making industry. *Sci. Tot. Environ.*, 511-512, 411-420.
751
752 AQEG, 2011. Air Quality Expert Group. Understanding PM₁₀ in Port Talbot. Advice note
753 prepared for Department of Environment, Food and Rural Affairs: Scottish, Welsh
754 Assembly Government, and Department of the Environment, Northern Ireland.
755
756 Beddows, D.C.S., Dall'Osto, M., Harrison, R.M., 2009. Cluster analysis of rural, urban and
757 curbside atmospheric particle size data. *Environ. Sci. Technol.*, 43, 4694-4700.
758
759 Carslaw, D.C. and Ropkins, K., 2012. *Openair* - an R package for air quality data
760 analysis. *Environ. Modell. Softw.*, 27-28, 52-61.
761
762 Dall'Osto, M., Booth, M.J., Smith, W., Fisher, R., R.M. Harrison, 2008a. A study of the
763 size distributions and the chemical characterisation of airborne particles in the vicinity of a
764 large integrated steelworks. *Aerosol Sci. Technol.*, 42, 981-991.
765
766 Dall'Osto, M., Booth, M.J., Smith, W., Fisher, R. and Harrison, R.M., 2008b. A study of the
767 size distributions and the chemical characterisation of airborne particles in the vicinity of a
768 large integrated steelworks. *Aerosol Sci. Technol.*, 42, 981-991.
769
770 Dall'Osto, D., Drewnick, F., Fisher, R., Harrison, R.M., 2012a. Real-time measurements of
771 nonmetallic fine particulate matter adjacent to a major integrated steelworks. *Aerosol Sci.*
772 *Technol.*, 46, 6, 639-653.
773
774 Dall'Osto, M., Drewnick, F., Fisher, R., Harrison R.M., 2012b. Real-time measurements of
775 non-metallic fine particulate matter adjacent to a major integrated steelworks. *Aerosol Sci.*
776 *Technol.*, 46, 639-653.
777
778 Ebert, M., Müller-Ebert, D., Benker, N., Weinbruch, S., 2012. Source apportionment of
779 aerosol near a steel plant by electron microscopy. *J. Environ. Monit.*, 14, 3257-3266.
780
781 Environment Agency Wales, 2009. Port Talbot Steelworks PM Permit Review.
782
783 Gladtko, D., Volkhausen, W., Bastian, B., Estimating the contribution of industrial facilities
784 to annual PM₁₀ concentrations at industrially influenced sites. *Atmos. Environ.* 43 (2009)
785 4655–4665.
786
787 Guinot, B., Gonzalez, B., Perim De Faria, J., and Kedia, S., Particulate matter
788 characterization in a steelworks using conventional sampling and innovative lidar
789 observations. *Particuology* 28 (2016) 43–51.
790
791 Hayes, E. and Chatterton, T., 2009. An independent review of monitoring measures
792 undertaken in Neath Port Talbot in respect of particulate matter (PM₁₀), Report prepared
793 for the Welsh Assembly Government by the University of the West of England, Bristol.
794

- 795 Hleis, D., Fernández-Olmo, I., Ledoux, F., Kfoury, A., Courcot, L., Desmonts, T., and
796 Courcot, D., Chemical profile identification of fugitive and confined particle emissions from
797 an integrated iron and steelmaking plant. *Journal of Hazardous Materials* 250– 251 (2013)
798 246–255.
- 799
- 800 Johansson, M.T., Söderström, M., 2011. Options for the Swedish steel industry - Energy
801 efficiency measures and fuel conversion. *Energy*, 36, 191-198.
- 802
- 803 Kfoury, A., Ledoux, F., Roche, C., Delmaire, G., Roussel, G. and Courcot, D. PM 2.5
804 source apportionment in a French urban coastal site under steelworks emission influences
805 using constrained non-negative matrix factorization receptor model, *J. Environ. Sci.*, 40
806 (2016) 114–128.
- 807
- 808 Laxen, D., Moorcroft, S., Marnier, B., Laxen, K., Boulter, P., Barlow, T., Harrison, R.M.,
809 Heal, M., 2010. PM_{2.5} in the UK. Project ER12 Final Report.
810 www.aqconsultants.co.uk/AQC/.../Reports/SNIFFER-PM25-Rept-Final-201210.pdf [Last
811 accessed 18 Aug 2017].
- 812
- 813 Lucarelli, F., Nava, S., Calzolari, G., Chiari, M., Udisti, R., Marino, F., 2011. Is PIXE still a
814 useful technique for the analysis of atmospheric aerosols? *The LAB Experience. X-Ray*
815 *Spectrom.*, 40, 162-167.
- 816
- 817 Macheimer, S., D., 2004. Characterization of airborne and bulk particulate from iron and
818 steel manufacturing facilities. *Environ. Sci. Technol.*, 38, 381-389.
- 819
- 820 Met Office, 2012. Met Office Integrated Data Archive System (MIDAS) Land and Marine
821 Surface Stations Data (1853-current). NCAS British Atmospheric Data Centre, date of
822 citation, 2012. <http://catalogue.ceda.ac.uk/uuid/220a65615218d5c9cc9e4785a3234bd0>
823 [Last accessed 18 Aug 2017].
- 824
- 825 Moreno, T., Jones, T.P. and Richards, R.J., 2004. Characterisation of aerosol particulate
826 matter from urban and industrial environments: examples from Cardiff and Port Talbot,
827 South Wales, UK. *Sci. Total Environ.*, 334-335, 337-346.
- 828
- 829 Oravisjarvi, K., Timonen, K.L., Wiikinkoski, T., Ruuskanen, A.R., Heinanen, K.,
830 Ruuskanen, J., 2003. Source contributions to PM_{2.5} particles in the urban air of a town
831 situated close to a steel work. *Atmos. Environ.*, 37, 1013-1022.
- 832
- 833 Sylvestre, A., Mizzi, A., Mathiot, S., Masson, F., Jeffrezo, J.L., Dron, J., Mesbah, B.,
834 Wortham, H., Marchand, N., 2017. Comprehensive chemical characterization of industrial
835 PM_{2.5} from steel industry activities, *Atmos. Environ.*, 152, 180-190.
- 836
- 837 Taiwo, A., Beddows, D., Calzolari, G., Harrison, R.M., Lucarelli, F., Nava, S., Shi, Z., Valli,
838 G. and Vecchi, R., 2014a. Receptor modelling of airborne particulate matter in the vicinity
839 of a major steelworks site. *Sci. Tot. Environ.*, 490, 488-500.
- 840
- 841 Taiwo, A.M., Harrison, R.M., Beddows, D.C., Shi, Z., 2014b. Source apportionment of
842 single particles sampled at the industrially polluted town of Port Talbot, United Kingdom by
843 ATOFMS. *Atmos. Environ.*, 97, 155-165.
- 844

- 845 Taiwo, A.M., Beddows, D.C.S., Shi, Z., Harrison, R.M., 2014c. Mass and number size
846 distributions of particulate matter components: Comparison of an industrial site and an
847 urban background site. *Sci. Tot. Environ.*, 475, 29-38.
- 848
- 849 Tsai, J.-H., Lin, K.-H., Chen, C.-Y., Ding, J.-Y., Choa, C.-G. and Chiang, H.-L., 2007.
850 Chemical constituents in particulate emissions from integrated iron and steel facility. *J.*
851 *Hazard Mater.*, 147, 111-119.
- 852
- 853 Tsai, J.-H., Lin, K.H., Chen, C.-Y., Lai, N., Ma, S.Y. and Chiang, H.-L., 2008. Volatile
854 organic compound constituents from an integrated iron and steel facility. *J. Hazard.*
855 *Mater.*, 157, 569-578.
- 856
- 857 Uria-Tellaetxe, I., Carslaw, C.D., 2014. Conditional bivariate probability function for source
858 identification. *Environ. Modell. Softw.* 59, 1-9.
- 859
- 860

861
862
863
864
865
866
867
868
869
870
871
872
873
874
875
876
877
878
879
880
881
882
883
884
885
886
887
888
889
890
891
892
893
894
895
896
897
898
899
900
901
902
903
904
905
906
907
908
909

TABLE LEGENDS

Table 1 Monitoring sites placed around the perimeter of Port Talbot steelworks (2012).

Table 2 Instrument Augmentation by Birmingham University (May 2012).

FIGURE LEGENDS

Figure 1 Map of Port Talbot showing the sources areas. The black targets indicate the positions of the monitoring site listed in Table 1. Modified from Laxen et al., 2010.

Figure 2 Maps showing the areas of potential sources creating high concentrations of PM₁₀ measured at the Little Warren (LW) and Port Talbot Margam AURN (FS) sites. The schematic shows the possible position of a line source relative to the LW and FS and the angles of high PM from this with $\alpha > \beta$. [Plotted using data measured during campaign 18 April-16 May 2012. Red and blue lines mark the 95 and 90 percentile directions respectively, , PM₁₀ units: $\mu\text{g}/\text{m}^3$].

Figure 3 Wind roses identifying the cross sectioned area on the map as an area of most likely sources of PM₁₀ that contribute to high concentrations. [Plotted using data measured during campaign 18 April-16 May 2012, PM₁₀ units: $\mu\text{g}/\text{m}^3$]. Upper diagram shows the triangulation (using wind directions with PM₁₀ greater than the 90th percentile) used to prescribe the source area and the lower diagram shows the aerial photograph of the area. [Little Warren (LW), Port Talbot Margam AURN (FS), Port Talbot Docks (DOCKS), Prince Street (PS), Twll-yn-y-Wall (Twll) and Dyffryn School (DS) sites].

Figure 4 Comparison of maximum PM₁₀ measured at the six sites (FS-Fire Station; LW-Little Warren; DS – Dyffryn School; DOCK –Port Talbot Docks; PS – Prince Street; Twll – Twll-yn-y-Wal). The colours show what the fraction of the height of the bar represents the frequency of occurrence of the PM₁₀ range of values. [Plotted using data measured during campaign 18 April-16 May 2012].

Figure 5 Comparison of PM₁₀ measured at the six sites (FS-Fire Station; LW-Little Warren; DS – Dyffryn School; DOCK –Port Talbot Docks; PS – Prince Street; Twll – Twll-yn-y-Wal] around Port Talbot. Mean and maximum values plotted against distance from the centre of the Slag Handling area (*lat* = $51^{\circ}, 34', 16.154''N$, *long* = $3^{\circ}, 46', 57.648''W$, -). [Plotted using data measured during campaign 18 April-16 May 2012.16 May 2012]. (a) mean PM10; (b) maximum PM10; (c) 90%th percentile PM₁₀].

Figure 6 Conditional probability wind roses showing (a) the 75-100 percentile range of PM₁₀ values (LW = 23-99 and FS = 27-210 $\mu\text{g}/\text{m}^3$) (b) the 0-75 percentile range of PM₁₀ values (LW = 0-23 and FS = 0-27 $\mu\text{g}/\text{m}^3$). [Colour scale

- 910 represents the conditional probability from 0 to 1 as colours from blue
911 through to red].
912
- 913 **Figure 7** Bar chart showing the elemental composition of the average PM_{10} value for
914 four ranges spanning the full range of (a) PM_{10} concentrations and (b) Wind
915 speed measured at the Fire Station AURN site. [Grey hatched area indicates
916 the fraction of the PM_{10} not accounted for by the Streaker measurements].
917 [Units: $\mu\text{g}/\text{m}^3$] [Quartile range of wind speeds used, m/s].
918
- 919 **Figure 8** Bar charts showing the composition as described by ME2 factors by Taiwo et
920 al. (2014a) of the average PM_{10} concentrations for four ranges spanning (a)
921 the full range of PM_{10} concentrations and (b) wind speed measured at the
922 Fire Station AURN site. [Grey hatched area indicates the fraction of the PM_{10}
923 not accounted for by the Streaker measurements]. [Quartile PM_{10} and speed
924 ranges used, $\mu\text{g}/\text{m}^3$, m/s].
925
- 926 **Figure 9** Analysis of Grimm data: (a) map showing sectors representing the
927 steelworks and background; (b) number size distribution [units: $1/\text{cm}^3$]; (c)
928 volume size distribution [units: $\mu\text{m}^3/\text{cm}^3$].
929
- 930 **Figure 10** (a) Relationship between area under the curves to measured mean PM_{10} ; (b)
931 same data plotted for individual modes within the Grimm size distribution
932 data. Two largest modes with modal diameters at 2.2 and 4.5 μm have the
933 highest correlation with PM_{10} and have been associated with an FeP particle
934 type from Hot and Cold Mills by Dall'Osto et al. (2008b).). [units: $dV/d\text{Log}D_p$
935 - $\mu\text{m}^3/\text{cm}^3$].
936
937

938 **Table 1.** Monitoring sites placed around the perimeter of Port Talbot steelworks (2012).

ACCEPTED MANUSCRIPT

Site	Lat	Long	*PM ₁₀	*PM _{2.5}	O ₃	SO ₂	CO	NO _x	NO ₂	NO	Met
Little Warren (LW)	51 : 35' : 5.748" N	3 : 48' : 3.848" W	✓19 µg m ⁻³								✓**
Port Talbot Docks (DOCKS)	51 : 35' : 24.839" N	3 : 47' : 9.776" W	✓18 µg m ⁻³								
Talbot Road	51 : 35' : 29.324" N	3 : 46' : 45.109" W	✓22 µg m ⁻³								
Theodore Road	51 : 35' : 23.791" N	3 : 46' : 19.218" W	✓19 µg m ⁻³								
Margam Fire Station (FS)	51 : 35' : 2.220" N	3 : 46' : 14.959" W	✓23 µg m ⁻³	✓	✓	✓	✓	✓	✓	✓	✓
Prince Street (PS)	51 : 34' : 46.762" N	3 : 45' : 59.274" W	✓23 µg m ⁻³	✓							
Twl-yn-y-Wal Park (TWLL)	51 : 34' : 36.034" N	3 : 45' : 32.418" W	✓23 µg m ⁻³								
Dyffryn School (DS)	51 : 34' : 20.759" N	3 : 45' : 3.931" W	✓16 µg m ⁻³								
Mumbles Head (MU)	51 : 33' : 54.000" N	3 : 58' : 51.600" W									✓

*PM10 measured with TEOM FDMS and hence split into non-volatile and volatile fraction. Figure next to tick mark is the Annual Mean for 2012.

Annual mean for 2016 given for PS.

** Modelled data.

939

940 **Table 2.** Instrument Augmentation by Birmingham University (May 2012).

Site	Partisol 2025	PCR TECTORA Streaker	Digitel DHA-80	ATOFMS TSI 3800	Aethalometer AE31	GRIMM Dust Monitor v1.108
Little Warren (LW)	✓	✓				
Margam Fire Station (FS)	✓	✓	✓	✓	✓	✓
Prince Street (PS)	✓					
Dyffryn School (DS)	✓					

941

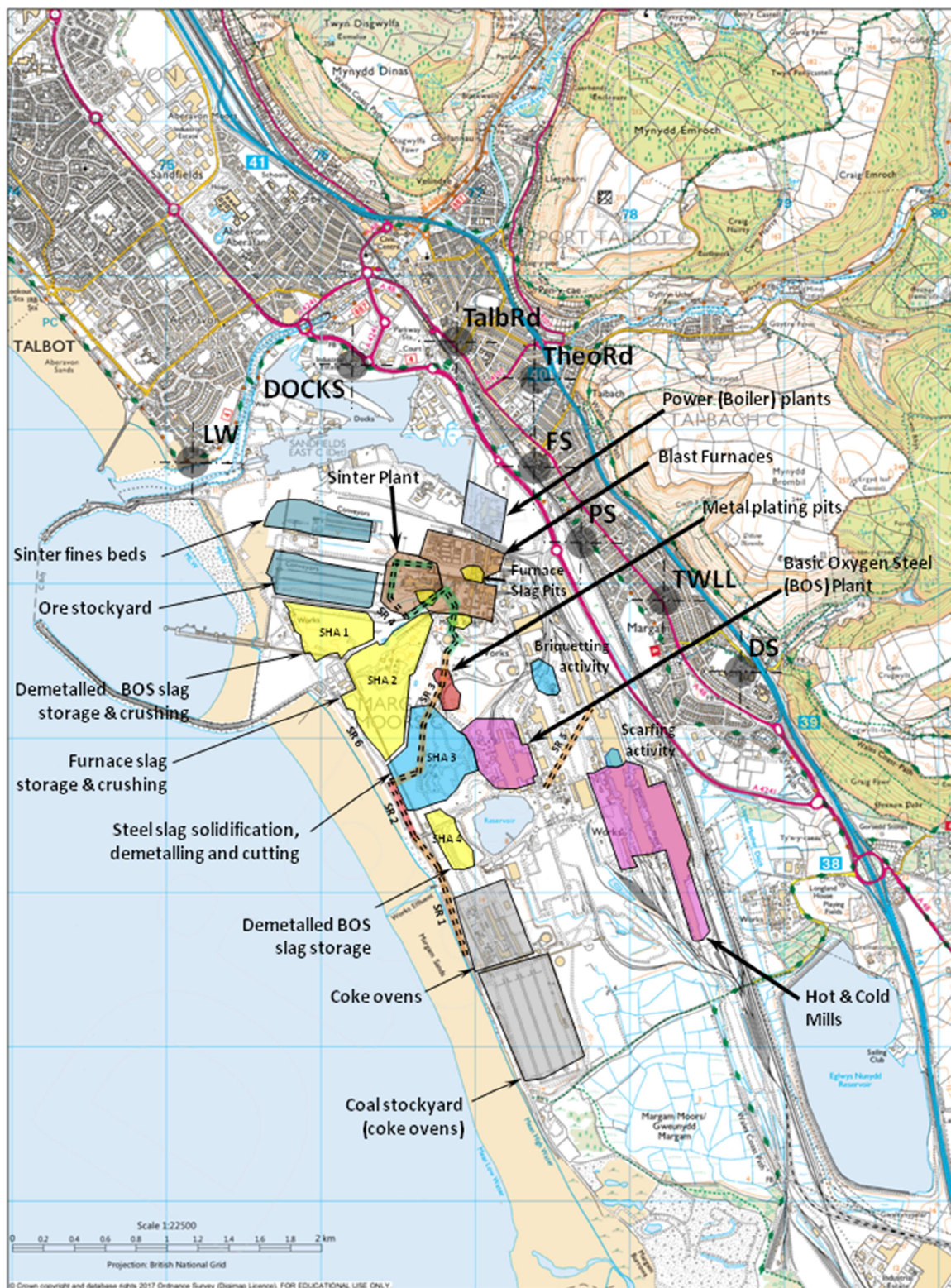
942

943 **Table 3.** Summary of ATOFMS clusters derived using ART2a analysis.

944

Cluster Number	Type	Characteristic	% Counts	Comments
1	K-NO ₃	Regional Nitrate	25.1	Local and NE winds
2	EC	Regional EC	31.5	Local
3	NaCl	Sea Salt	9	Local
4	NaK-CN	Dust?	8.5	Local and W Winds
5	KSO ₄	Regional Sulphate	5	Local and W Winds
6	PAH	PT	7.5	S winds, no clear diurnal trend
7	FePO ₃	PT Phosphate	7.5	S winds, peaks at 6am and 1pm
8	SOA	Traffic	2	NE Winds, strong at night.
9	Ca-EC	Lub oil from roads	1	SW winds, high during 6:00-21:00.
10	FeNO _x	FeNit	0.6	Local, strong at 5am.
11	K-EC	Traffic	0.6	NE winds, strong in afternoon and evening
12	K-SO ₄	Traffic	0.6	NE winds, strong in afternoon and evening
13	KCl – Unique	PT Chloride	0.5	SW winds, no clear diurnal trend
14	Amines	Amines 24hr episode	0.4	SW winds, no clear diurnal trend
15	Copper	PT – Copper	0.1	SW winds, Strong at 4-5am.
16	Sulphur	PT – Sulphur	0.1	Local and SW winds, strong at midday.

945



© Crown Copyright/database right 2011. An Ordnance Survey EDINA supplied service.

Figure 1. Map of Port Talbot showing the sources areas. The black targets indicate the positions of the monitoring site listed in Table 1. Modified from Laxen et al., 2010.

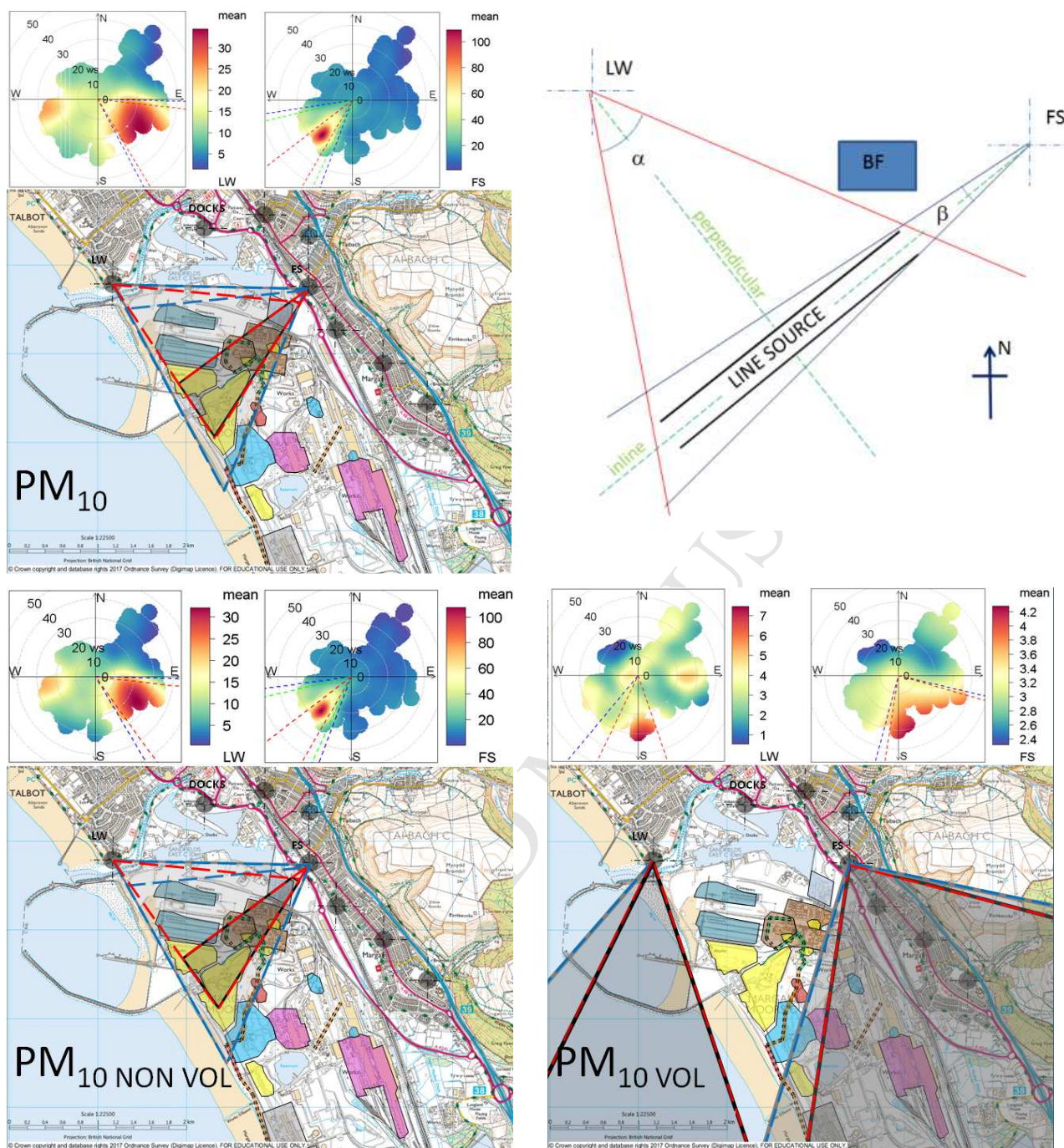
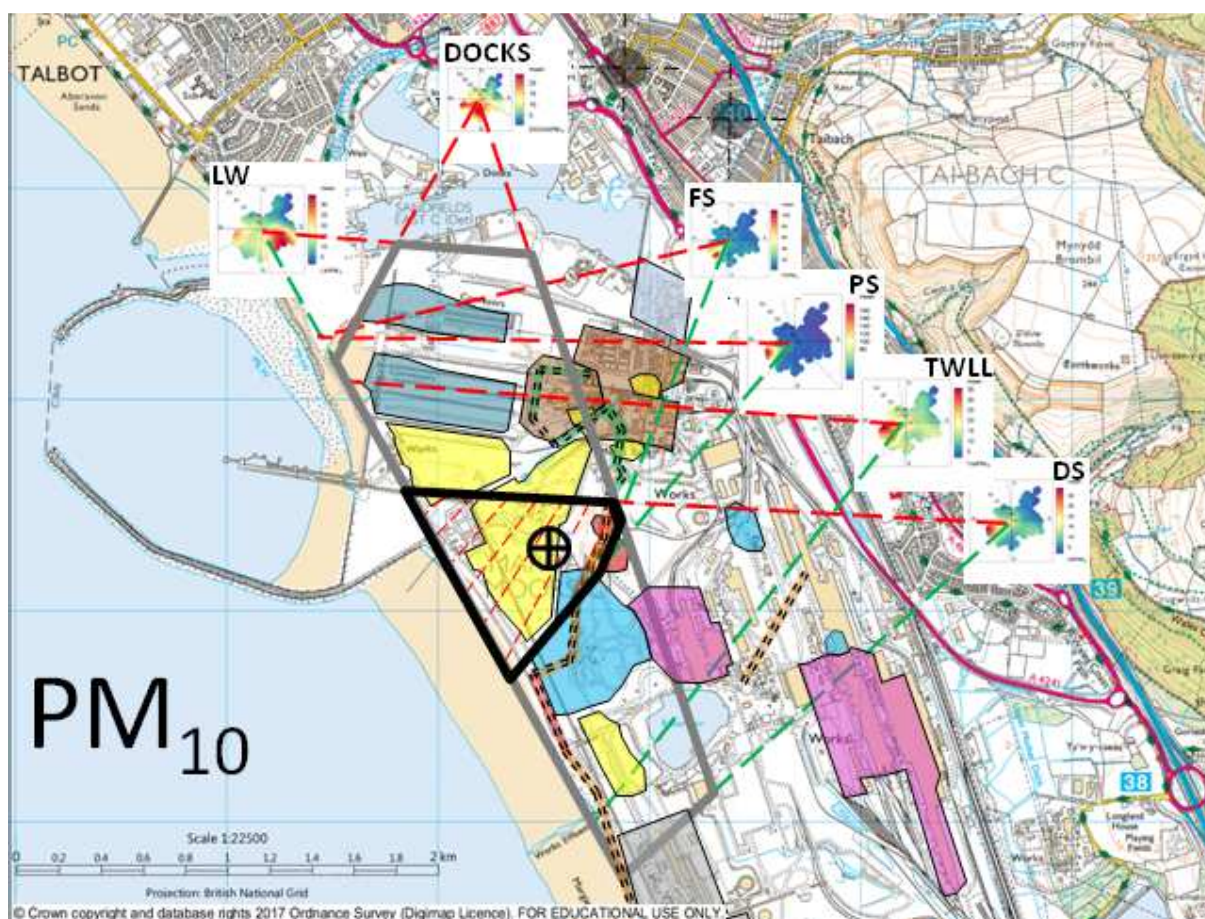


Figure 2. Maps showing the areas of potential sources creating high concentrations of PM₁₀ measured at the Little Warren (LW) and Port Talbot Margam AURN (FS) sites. The schematic shows the possible position of a line source relative to the LW and FS and the angles of high PM from this with $\alpha > \beta$. [Plotted using data measured during campaign 18 April-16 May 2012. Red and blue lines mark the 95 and 90 percentile directions respectively. PM₁₀ units: $\mu\text{g}/\text{m}^3$].

946
947



<https://www.google.co.uk/maps/@51.571154,-3.78268,16z>

Figure 3. Wind roses identifying the cross sectioned area on the map as an area of most likely sources of PM₁₀ that contribute to high concentrations. [Plotted using data measured during campaign 18 April-16 May 2012, PM₁₀ units: $\mu\text{g}/\text{m}^3$]. Upper diagram shows the triangulation (using wind directions with PM₁₀ greater than the 90th percentile) used to prescribe the source area and the lower diagram shows the aerial photograph of the area. [Little Warren (LW), Port Talbot Margam AURN (FS), Port Talbot Docks (DOCKS), Prince Street (PS), Twll-yn-y-Wall (Twll) and Dyffryn School (DS) sites].

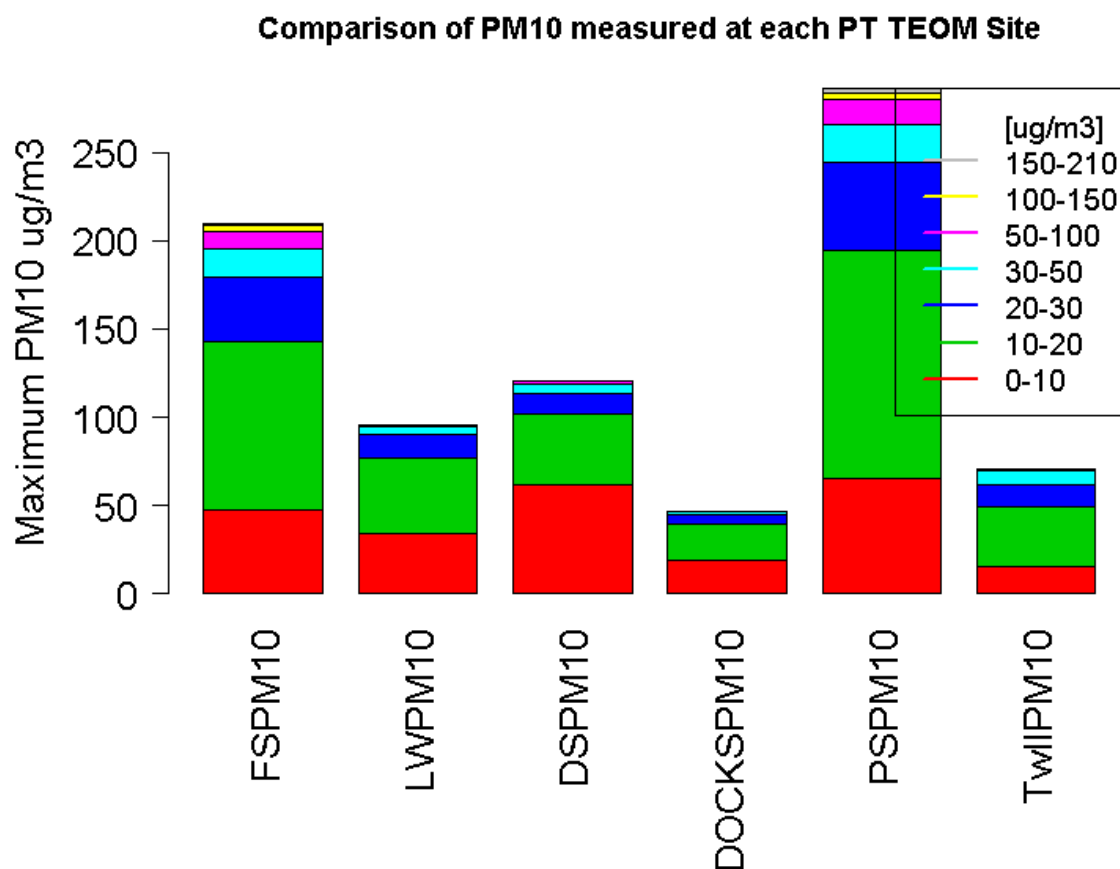


Figure 4. Comparison of maximum PM₁₀ measured at the six sites (FS-Fire Station; LW-Little Warren; DS – Dyffryn School; DOCK –Port Talbot Docks; PS – Prince Street; Twll – Twll-yn-y-Wal). The colours show what the fraction of the height of the bar represents the frequency of occurrence of the PM₁₀ range of values. [Plotted using data measured during campaign 18 April-16 May 2012].

949
950
951
952
953
954
955
956
957
958
959

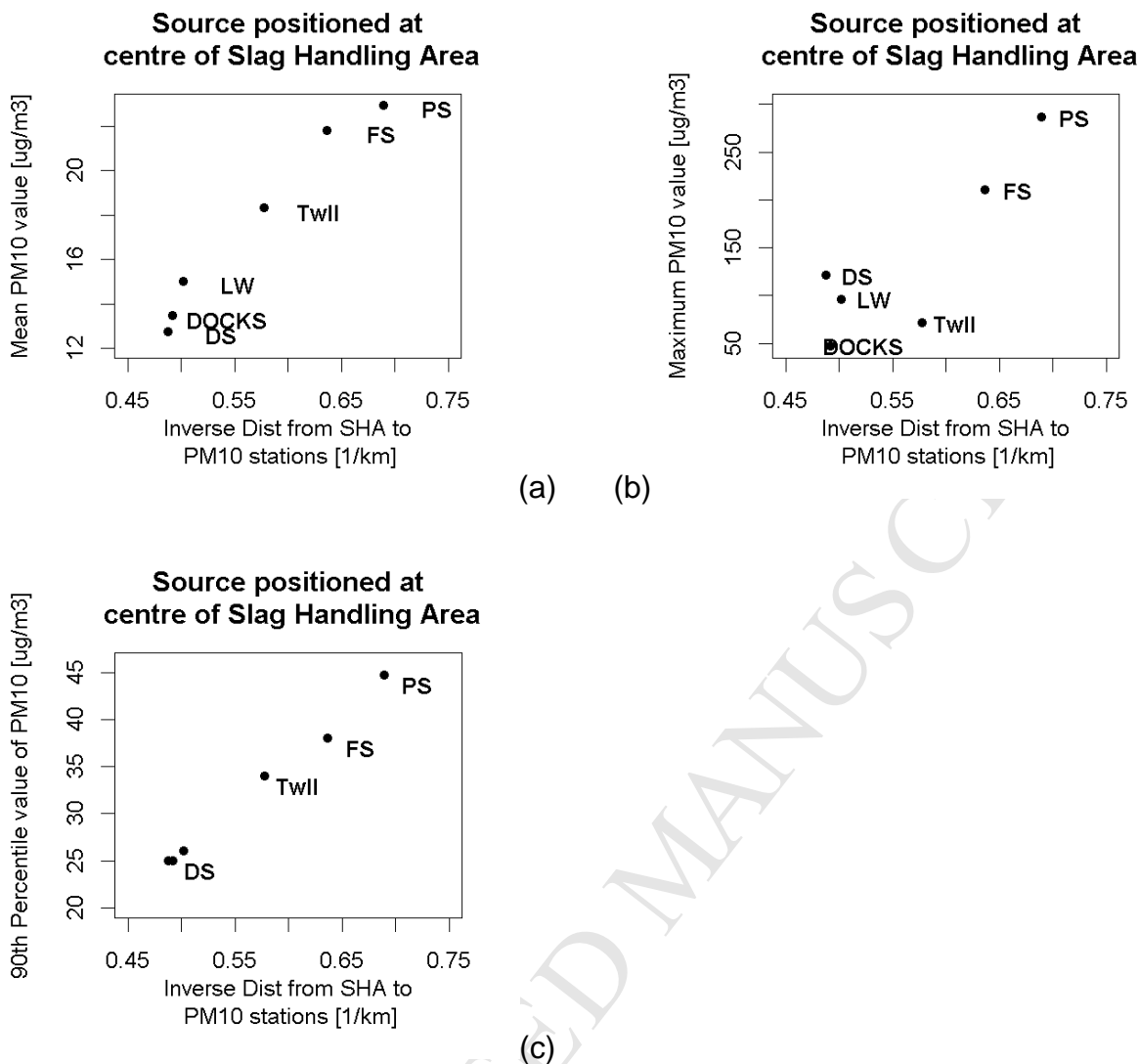


Figure 5. Comparison of PM_{10} measured at the six sites (FS-Fire Station; LW-Little Warren; DS – Dyffryn School; DOCK –Port Talbot Docks; PS – Prince Street; Twll – Twll-yn-y-Wal] around Port Talbot. Mean and maximum values plotted against inverse distance (1/km) from the centre of the Slag Handling area ($lat = 51^{\circ},34',16.154''N$, $long = 3^{\circ},46', 57.648''W$). [Plotted using data measured during campaign 18 April-16 May 2012.16 May 2012]. (a) mean PM_{10} ; (b) maximum PM_{10} ; (c) 90%th percentile PM_{10} .]

960
961
962
963
964

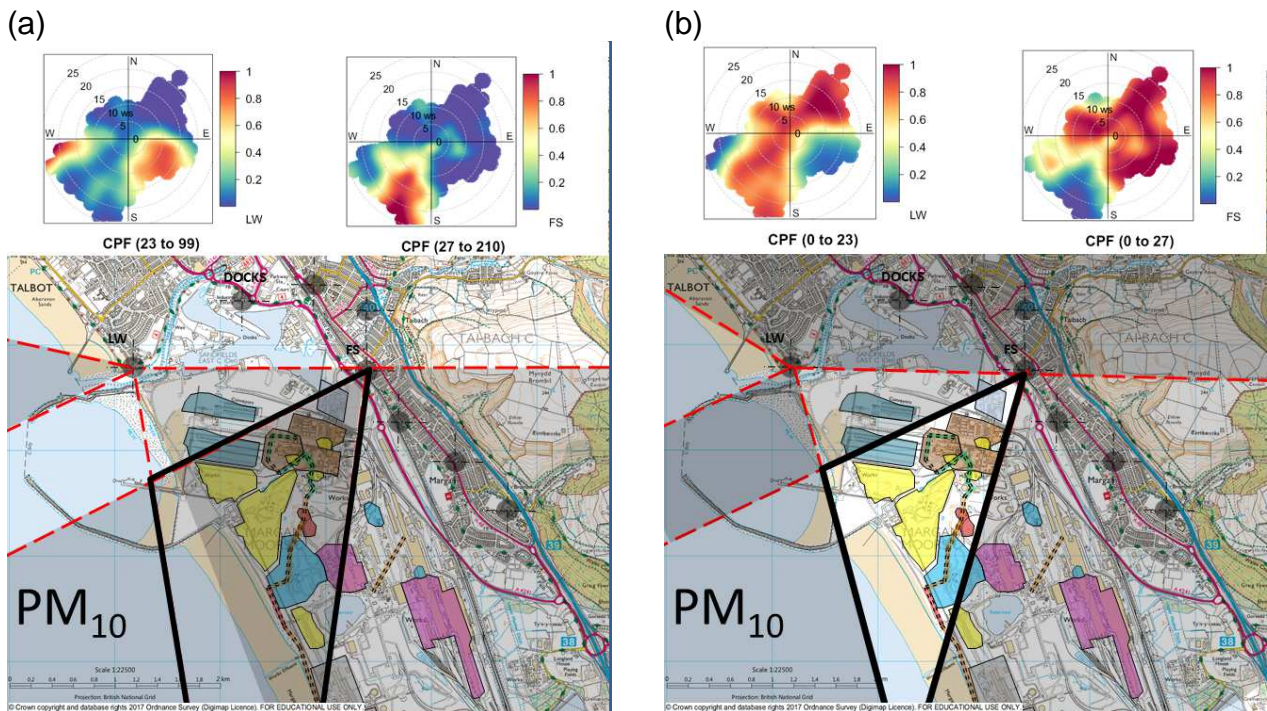


Figure 6. Conditional probability wind roses showing (a) the 75-100 percentile range of PM_{10} values ($LW = 23-99$ and $FS = 27-210 \mu g/m^3$) (b) the 0-75 percentile range of PM_{10} values ($LW = 0-23$ and $FS = 0-27 \mu g/m^3$). [Colour scale represents the conditional probability from 0 to 1 as colours from blue through to red].

965
966
967

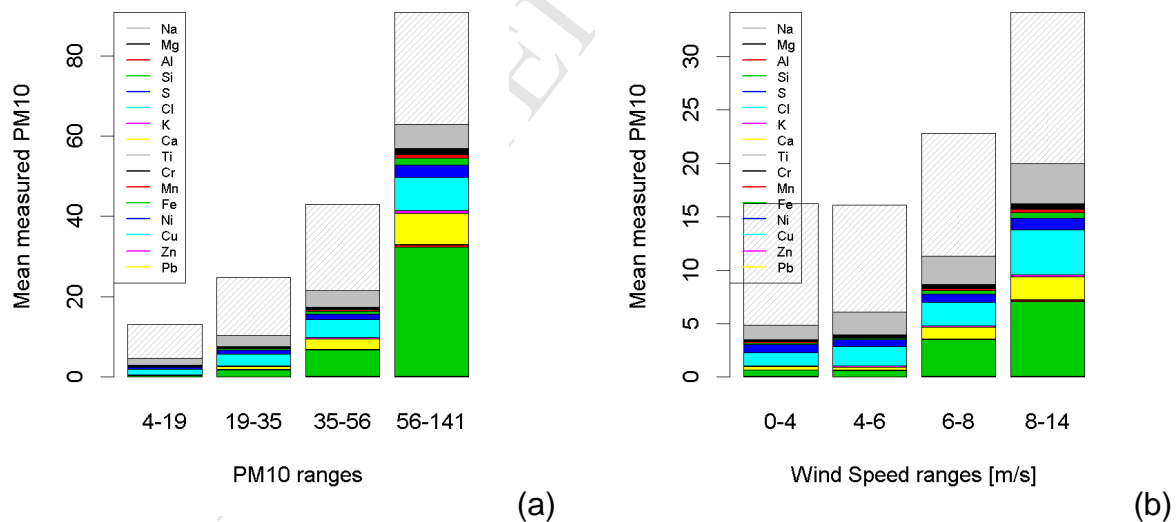


Figure 7. Bar chart showing the elemental composition of the average PM_{10} value for four ranges spanning the full range of (a) PM_{10} concentrations and (b) Wind speed measured at the Fire Station AURN site. [Grey hatched area indicates the fraction of the PM_{10} not accounted for by the Streaker measurements]. [PM_{10} units: $\mu g/m^3$] [Quartile range of wind speeds used, m/s].

968
969

970

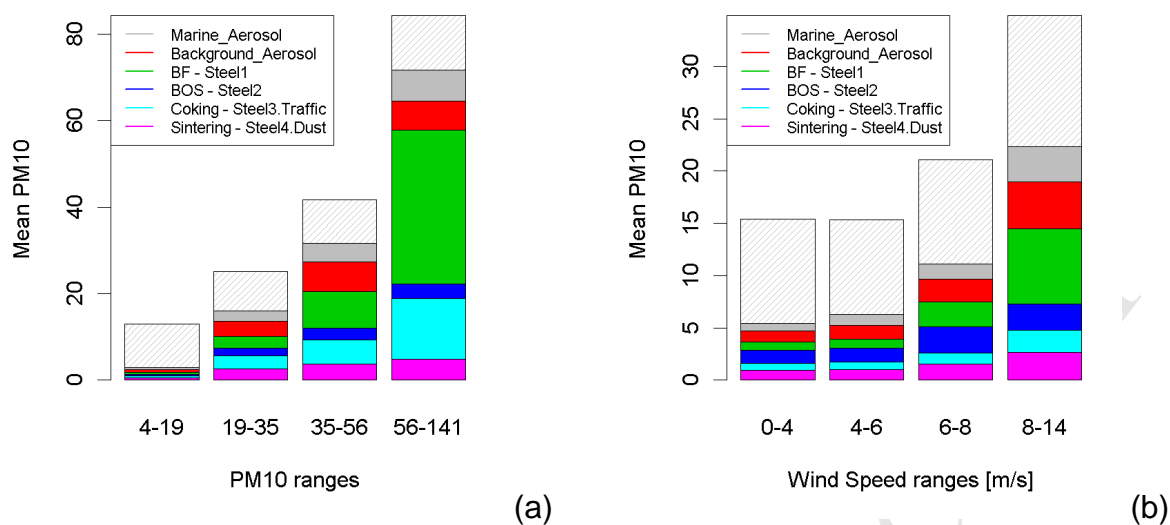
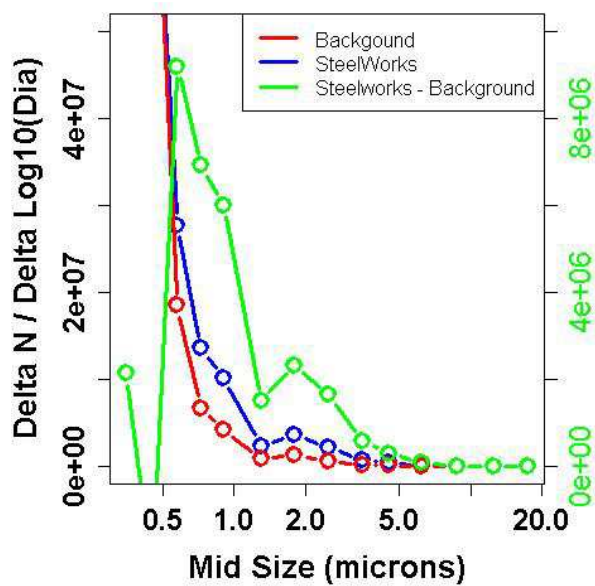
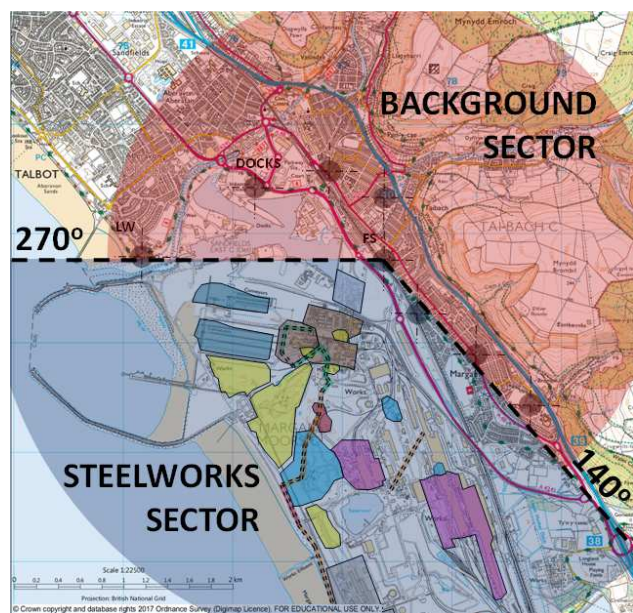


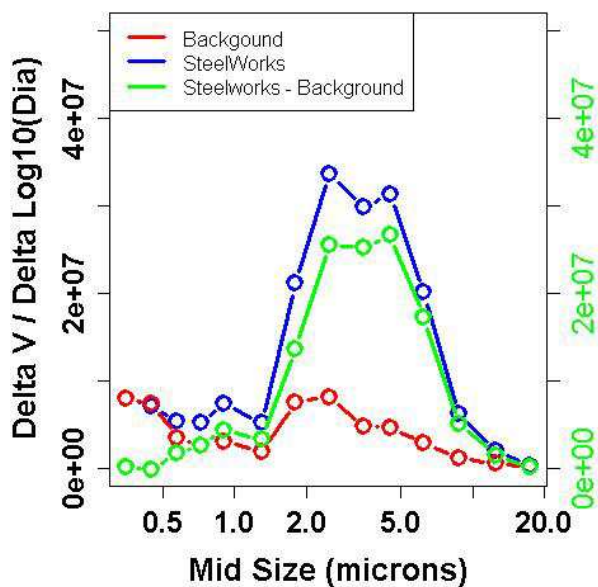
Figure 8. Bar charts showing the composition as described by ME2 factors by Taiwo et al. (2014a) of the average PM_{10} concentrations for four ranges spanning (a) the full range of PM_{10} concentrations and (b) wind speed measured at the Fire Station AURN site. [Grey hatched area indicates the fraction of the PM_{10} not accounted for by the Streaker measurements]. [Quartile PM_{10} and speed ranges used, $\mu g/m^3$, m/s].

971
 972
 973
 974
 975
 976
 977
 978
 979
 980
 981
 982
 983
 984



b

a



c

Figure 9. Analysis of Grimm data: (a) map showing sectors representing the steelworks and background; (b) number size distribution [units: $1/\text{cm}^3$]; (c) volume size distribution [units: $\mu\text{m}^3/\text{cm}^3$].

985
986
987
988
989
990
991
992

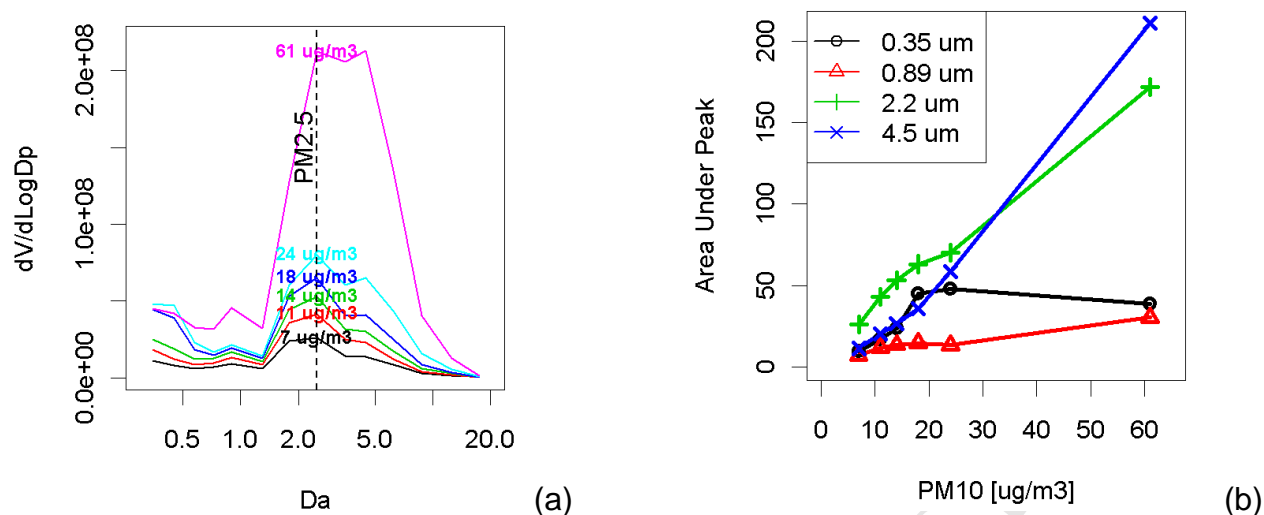


Figure 10. (a) Relationship between area under the curves to measured mean PM₁₀; (b) same data plotted for individual modes within the Grimm size distribution data. Two largest modes with modal diameters at 2.2 and 4.5 µm have the highest correlation with PM₁₀ and have been associated with an FeP particle type from Hot and Cold Mills by Dall'Osto et al. (2008b). [units: dV/dLogDp - µm³/cm³].

993
994

Identification of Specific Sources of Airborne Particles emitted from within a Complex Industrial (Steelworks) Site

D.C.S. Beddows and Roy M. Harrison

HIGHLIGHTS

- Contributions of a steelworks to PM mass are assessed
- Directional analysis identifies slag handling as a major source
- Wind-driven resuspension generates coarse particles
- Chemical composition at upwind and downwind sites defines sources
- Correlation of PM with SO₂ is due to a process emission source